Overcoming MET-targeted drug resistance in *MET*-amplified lung cancer by Aurora Kinase B inhibition

Yu-Ra Choi

Department of Medical Science

Graduate School

Yonsei University

Overcoming MET-targeted drug resistance in *MET*-amplified lung cancer by Aurora Kinase B inhibition

Advisor Jae J. Song

A Dissertation Submitted
to the Department of Medical Science
and the Committee on Graduate School
of Yonsei University in Partial Fulfillment of the
Requirements for the Degree of
Doctor of Philosophy in Medical Science

Yu-Ra Choi

January 2025

This certifies that the Dissertation of Yu-Ra Choi is approved

Thesis Supervisor Jae J. Song

Thesis Committee Member Youngjoo Lee

Thesis Committee Member Minkyu Jung

Thesis Committee Member Eun Young Kim

Thesis Committee Member Yang-Gun Suh

The Graduate School
Yonsei University

January 2025

Acknowledgments

During six years of doctoral study, I often imagined the moment I would defend my thesis and write a 'thank you' note. I would be lying if I said I was not eager to complete my PhD program. Though the day seemed distant, I looked forward to it, contemplating what I would say and to whom, and how I would feel. This anticipation helped me forget the challenges of my studies for a time. There are countless people to whom I owe my deepest gratitude throughout this journey. Attempting to capture six years of experience on a few pages feels even more difficult than writing the thesis itself. Nevertheless, I wish to express my sincere thanks here, however briefly.

First and foremost, I am profoundly grateful to Dr. Youngjoo Lee, my advisor for the past seven years. Under her guidance, I have had the opportunity to reflect on myself and grow continuously throughout this long program. From February 2016, when I first arrived at the National Cancer Center as a fresh Master’s graduate, to now, as I prepare for marriage, I have grown immensely, not only as a researcher but also as a person, because of her unwavering support. She consistently encouraged me with fresh perspectives, offered comfort during moments of doubt, and illuminated the path forward. Dr. Lee was the first mentor I encountered in my professional life. She was my teacher and has become a trusted partner. Reflecting on the past decade of our association, many memories come to mind. When I first expressed my intention to pursue a PhD, she earnestly questioned whether I was prepared for the difficult road ahead. Throughout, she has been a source

of solace amid the stresses of work and interpersonal challenges. She shared her own experiences and trusted my efforts, even when experiments seemed impossible. She respected me both as a researcher and as a person, regardless of circumstances. I feel truly fortunate to have spent these invaluable years under her guidance and hold deep admiration and gratitude for her.

I also extend my heartfelt appreciation to Professors Jaejin Song, Minkyu Jung, Eun Young Kim, and Yang-Gun Suh, who served as members of my thesis committee. In particular, I am deeply thankful to Professor Jaejin Song for his unwavering support from the inception to the conclusion of this research. Our first meeting in January 2018 marked the beginning of a significant phase in my academic journey. I am grateful for his confidence in me as a student and his patience throughout this process.

Over the past ten years at the National Cancer Center, I have shared many joys and challenges with numerous colleagues. I would especially like to thank Dr. Tae-Sik Kim from the genome analysis team, Dr. SunShin Kim, for her assistance with various experiments, Dr. Hyoun Sook Kim for teaching me the value of respect and offering comfort during difficult times, and Jaemin Kim, with whom I continue to share support and encouragement. I am also grateful to Dabin Cheon, Sangheun Lee, Hayoung Kim, Yoonyoung Heo, and Yelin Joo, members of Dr. Hyoun Sook Kim's lab. Despite our different specialties, we have supported one another as researchers and discussed our challenges, and I deeply cherish their friendship. I would also like to acknowledge Hyeri, Jeongyeon, Jiwon, and Soojin, who are no longer with me at the National

Cancer Center but remain close friends. Additionally, I thank Dr. Jaehoon Lee and Dr. Taewook from the biochemistry lab at Yonsei University, where I completed my master's degree, for their invaluable help with challenging experiments.

Finally, I am deeply grateful to Eunjung, my best friend from high school through to the present, for her enduring support. I could not have completed this research without all these individuals who stood by me through times of uncertainty, sensitivity, and growth.

I am endlessly thankful to my family, whose love, faith, and support have sustained me every step of the way. I am grateful to my father, Sang-jin Choi, CEO of Chiak Spring Water, and my mother, Hee-sook Jung, a gifted guitarist, for exemplifying quiet strength and unconditional love. To my sister, pianist Bora Choi, and my brother-in-law, singer Hyun-ho Kim, I am thankful for the creativity and warmth they bring into my life. I also deeply appreciate my new family: my father-in-law Daehyun Kim, my mother-in-law Hye Kyung Shin, and my sister-in-law Yuri Kim, who welcomed me with open hearts and unwavering support. Above all, I thank my parents for their patience, belief, and love throughout every season of this journey. Their love is the foundation that allows me to stand tall wherever I go.

Lastly, I wish to express my heartfelt gratitude to my dearest friend, protector, and life partner, Tae Young Kim. Tae Young entered my life unexpectedly in February 2023, during a confusing and challenging time. His unwavering support, invaluable advice, and constant encouragement have been a source of strength throughout this long process. He was the first to make me feel truly

loved, and I am certain I could not have reached this point without him.

Looking back on this journey and all those who have supported me, I realize that there is no end to my gratitude. While I once believed that writing the thesis and graduation were the greatest challenges, I now understand that completing this entire process is the most demanding task. Though this message is too brief to fully repay the kindness I have received, I hope it conveys my heartfelt thanks to everyone who has stood by my side. Once again, thank you all sincerely.

TABLE OF CONTENTS

LIST OF FIGURES

LIST OF TABLES

ABSTRACT

Overcoming MET-targeted drug resistance in *MET*-amplified lung cancer by Aurora Kinase B inhibition

MET-targeted therapies are the most effective treatment for patients with *MET*-amplified lung cancer. However, acquired drug resistance is a significant challenge in *MET*-amplified lung cancer treatment. This study aimed to discover an effective treatment strategy for overcoming MET-targeted drug resistance. We first established a lung cancer cell line resistant to MET tyrosine kinase inhibitor (MET-TKI) (H1993 PR-S2) from *MET*-amplified lung cancer cells (H1993). High-throughput screening using an anti-cancer compound library identified Aurora Kinase B (AURKB) inhibitor as a potent agent suppressing H1993 PR-S2 cell viability. In these resistant cells, p-MET expression was markedly decreased, while p-AURKB was significantly increased. Furthermore, STAT3-activated gene signatures were enriched in H1993 PR-S2 cells, and p-STAT3 expression was closely linked to AURKB. The AURKB overexpression induced p-STAT3 activation in the parental cells, whereas the AURKB knockdown reduced p-STAT3 expression in the H1993 PR-S2 cells. The resistant cells showed increased BCL2 gene expression, and STAT3-BCL2 expression was highly suppressed by AURKB inhibitor. However, MET-TKI sensitivity was not enhanced by STAT3 or BCL2 knockdown in H1993 PR-S2 cells. Additionally, the elevated expression of cleavage-caspase3 and the G2/M phase arrest were observed at lower

concentrations of AURKB inhibitor in the H1993 PR-S2 cells. AURKB inhibitor also showed potent anti-tumor activity against the H1993 PR-S2 tumor xenografts. Finally, we confirmed the upregulated AURKB and p-STAT3 expression in post-treatment tumors of advanced *MET*-amplified lung cancer patient who experienced acquired resistance to MET-targeted drugs. These findings suggest AURKB is a potential druggable target for MET-TKI-resistant *MET*-amplified lung cancer treatment.

Keywords: lung cancer; *MET*-amplification; tyrosine kinase inhibitor; targeted therapy; drug resistance

1. Introduction

1.1. MET signaling

The hepatocyte growth factor receptor, also called *MET*, is a receptor tyrosine kinase (RTK) and is expressed on the cell surface as a transmembrane protein[1]. The MET pathway is activated by the binding of HGF and initiates various signaling cascades, including RAS/ERK, JAK/STAT3, and PI3K/AKT. MET activation is crucial in regulating cellular properties related to cell proliferation, survival, growth, invasion, and motility[2,3].

1.2. MET aberrations in NSCLC patients

The dysregulation of the MET pathway, a common occurrence in cancer, can arise through various mechanisms, including *MET* constitutive mutation, exon 14 skipping, amplification, gene fusion, and HGF overexpression[4,5]. Abnormal MET expression promotes cancer cell growth, rapid proliferation, tumor invasiveness, metastasis, chemotherapy resistance, and poor patient prognosis[6,7]. Recently, *MET* exon 14 skipping and *MET* amplification have been identified as major oncogenic drivers in non-small cell lung cancer (NSCLC)[8,9]. *MET* exon 14 skipping, caused by the loss of the juxtamembrane domain site of the *MET* gene, leads to reduced MET ubiquitination and increased cellular MET protein levels (Fig 1) [10]. According to

TCGA data analysis, *MET* exon 14 skipping is observed in 1.7 % to 4.3 % of primary NSCLC cases[11,12]. In contrast, *MET* amplification results from an increased copy number of the *MET* gene, leading to protein overexpression (Fig 1)[10], present in 1.0–5 % of patients with primary NSCLC[13]. Recent clinical studies have reported that *MET* amplification is a major driver of acquired resistance to tyrosine kinase inhibitors (TKIs), such as gefitinib for EGFR or lorlatinib for ALK[14], occurring in approximately 5–50 % of cases in patients who develop resistance[14]. Several studies have shown a correlation among *MET* exon 14 skipping, *MET* amplification, and the clinical outcomes of patients with NSCLC. Retrospective studies indicate that patients with advanced NSCLC with *MET* exon 14 skipping or *MET* amplification have worse overall survival than those without these alterations (hazard ratio; *MET* exon 14 skipping: 2.125 (95 % CI: 1.096–4.242); *MET* amplification: 3.444 (95 % CI: 1.398–8.482))[15]. These findings suggested that *MET* gene alterations are deeply involved in lung cancer development and may be important pivotal targets for lung cancer patients.

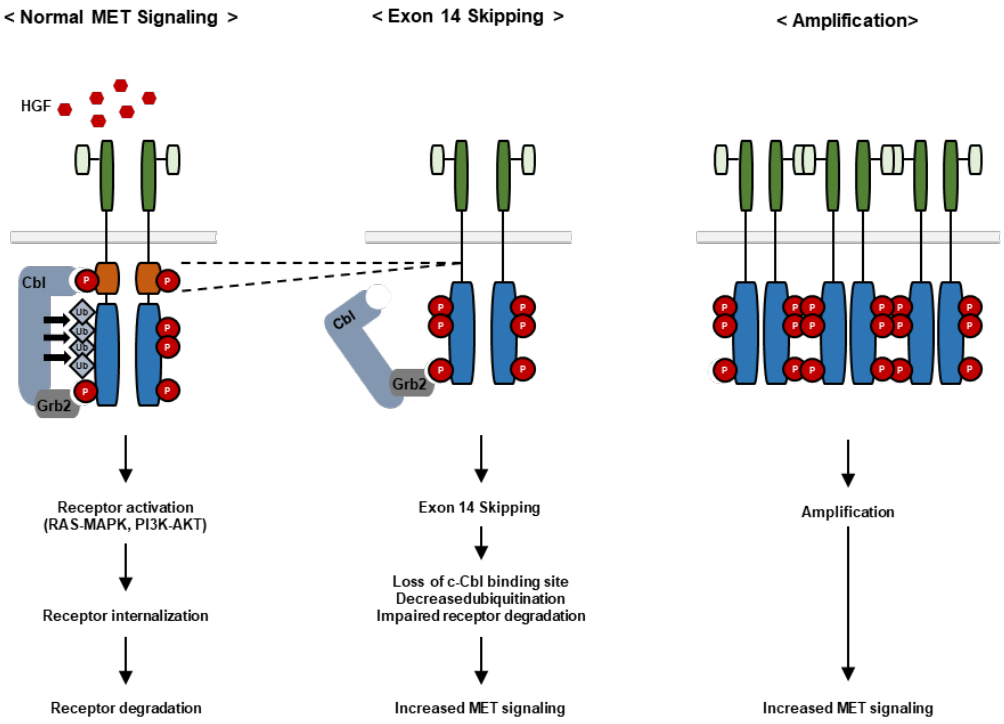

Fig 1. Models for *MET* exon 14 skipping and *MET* amplification. *MET* exon 14 contained the juxtamembrane domain and the binding site of E3 ubiquitin-ligase protein (Cbl). In normal MET signaling, Cbl binds to the site in exon 14, followed by MET receptor phosphorylation, and receptor internalization and degradation are induced. Skipping *MET* exon 14 inhibits this mechanism, resulting in impaired degradation and increased MET signaling cascade. Increased *MET* copy number variation upregulates activation of the MET pathway by highly increased MET phosphorylation.

1.3. MET-targeted therapies

Over several years, the development of inhibitors targeting the activated MET pathway has resulted in the emergence of several distinct inhibitor types, including TKIs, multikinase inhibitors, anti-MET antibodies, and anti-HGF antibodies (Fig 2)[16]. Among these, two representative MET-targeted inhibitors, capmatinib and tepotinib, have shown promising efficacy in treating NSCLC patients. Capmatinib, a selective small molecule MET inhibitor, has demonstrated anti-cancer effects in MET high-expressed *in vitro* and mouse xenograft models[17,18]. The GEOMETRY-mono 1 phase II clinical study evaluated the efficacy of capmatinib treatment in 43 treatment-naïve NSCLC patients with *MET* exon 14 skipping or *MET* amplification[19]. The capmatinib therapy showed promising results in this study. It showed a 68 % overall response rate (ORR), with progression-free survival (PFS) of 12.6 months and overall survival (OS) of 20.8 months for patients with *MET* exon 14 skipping[19]. For patients with *MET* amplification, the therapy showed a 40 % ORR and a 4.2-month PFS[19]. Another type I MET inhibitor, tepotinib is a highly selective ATP-binding blocker with promising clinical activity in advanced NSCLC patients with MET alterations[20]. The VISION phase II study evaluated the tepotinib treatment in 164 previously untreated NSCLC patients with *MET* exon 14 skipping[20]. In this study, the tepotinib therapy demonstrated significant efficacy with a 57.3 % ORR, 12.6 months PFS, and OS of 21.3 months[20]. Thus, these clinical findings currently highlight the therapeutic potential of targeting the MET pathway activation

in NSCLC patients with MET alterations.

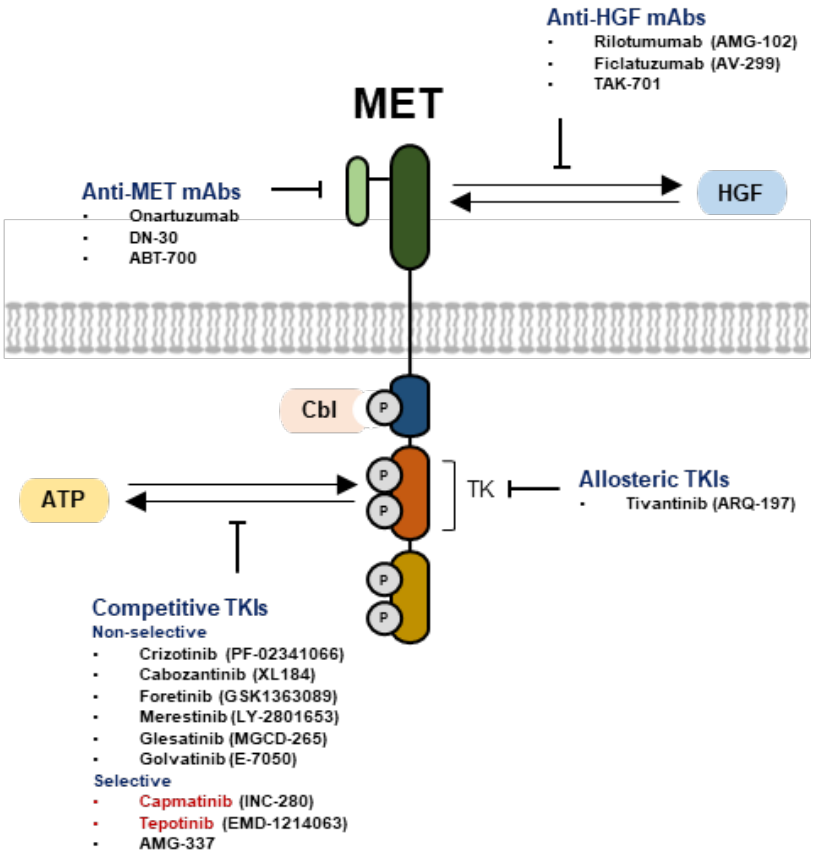

Fig 2. Representative HGF and MET signaling targeting agents. The target inhibitors of MET signaling can be assorted according to their action mechanisms: HGF ligand or the MET receptor targeting. HGF target agents are categorized into two groups: activation of HGF (pro-HGF cleavage inhibition) and HGF inhibitors (HGF direct interact inhibition). MET receptor target agents were categorized into two groups: MET antagonists (bind with the MET receptor without activating the signaling cascade) and MET tyrosine kinase inhibitors (ATP-binding site of the receptor and inhibit receptor transphosphorylation blocking).

1.4. Acquired resistance to MET-targeted therapy

However, unfortunately, despite the initial efficacy of MET-TKIs, patients treated with MET-targeted therapy experience resistance within approximately several months, and usually, a poor prognosis rapidly progresses. The NSCLC patients with MET alterations have exhibited resistance to MET-TKIs with 35 % on-target genetic mutations or 45 % off-target drug resistance mechanisms[21]. The MET-TKI such as capmatinib, tepotinib, and crizotinib treated patients harboring *MET* exon 14 skipping or *MET* amplification showed secondary point mutations such as D1228N and Y1230C of the *MET* kinase domain, resulting in drug resistance[22-24]. In a clinical study performed with 20 patients with *MET* exon 14 skipping, the researcher found that 7 patients had on-target genetic mutation plus *MET* amplification, and 9 patients had off-target molecular alteration including *KARS*, *EGFR*, and *HER3* amplification associated with drug resistance (Fig 3)[25]. Additionally, the preclinical results suggested MYC activation[26], *KRAS* amplification[27], and AKT/mTOR pathway activation[28] as MET-TKI acquired resistance mechanisms. Although several acquired resistance mechanisms have been reported for decades, a substantial portion of resistance to MET-TKI still remains unknown in NSCLC. Therefore, it is imperatively necessary to find effective treatment approaches to overcome this acquired resistance and prolong the survival of patients who have undergone MET-TKI treatment.

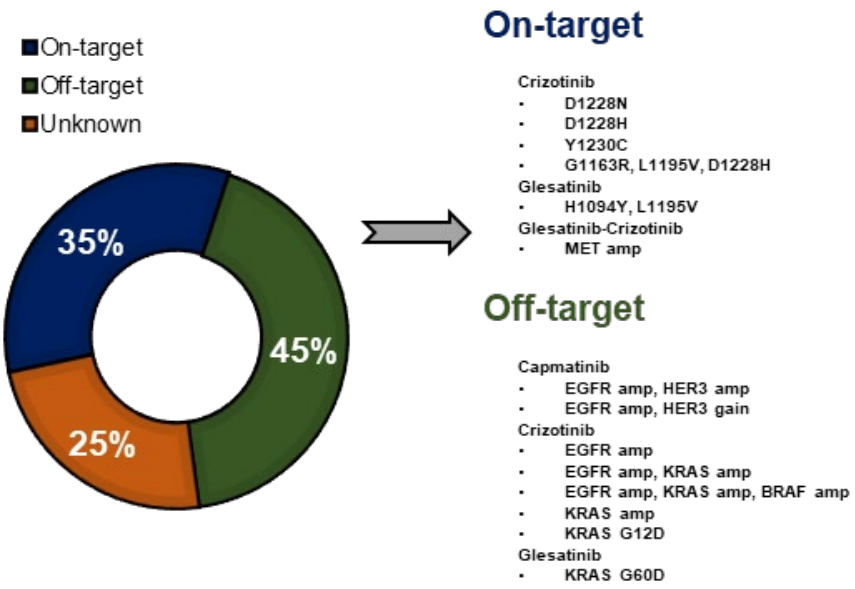

Fig 3. Genomic variation of MET-TKIs resistance patients. The research identified resistance mechanisms mediated by genomic alterations in 15 cases, representing 75 % of the cases examined. On-target variations (mutation of *MET* kinase domain or *MET* amplification) were identified in 7 samples (35 %). The *KRAS* mutations, or the amplification of *EGFR*, *HER3*, *BRAF*, and *KRAS*, as drug bypass mechanisms, were identified in 9 samples (45 %). Both on- and off-target resistance were exhibited in 1 sample, mutation of the D1228N *MET* kinase domain, and amplification of *EGFR* and *HER3* were observed. The genomic alterations of MET-TKI resistance mechanisms remained unidentified in 5 samples (25 %).

Therefore, the primary objective of this study was to elucidate novel mechanisms underlying acquired resistance to MET-TKI targeted therapy in *MET*-amplified NSCLC. In order to achieve this goal, we established *in vitro* models of acquired resistance by using MET-TKI-resistant lung cancer cell lines. Subsequently, we employed high-throughput drug screening methodology to identify potential therapeutic agents with the objective of developing effective anti-cancer therapies for MET-TKI acquired resistance. Our study aims to contribute to the development of effective treatment approaches and ultimately improve clinical outcomes for NSCLC patients who have *MET* amplification.

2. MATERIALS AND METHODS

2.1. Cell line and reagent

A549, H1975, and H1993 cell lines were obtained from the American Type Culture Collection (ATCC, Manassas, VA). The cell was maintained in RPMI-1640, a medium supplemented with 10 % fetal bovine serum. PHA665752, barasertib, VX680, MLN8237, AT9283, cycloheximide, and MG132 were purchased from Selleckchem Korea (Seoul, Korea).

2.2. Generation of MET-TKI acquired resistant cell line

MET-TKI-acquired resistant cells were established by treating the parental cell line with increasing concentrations of PHA665752 starting at 1 nM up to 1 μM. The MET-TKI acquired resistant cell line was maintained with 1 μM of PHA665752. The H1993 PR-S2 cell line was maintained in a drug-free medium for 1 week to perform all experiments.

2.3. Cell viability assay

The cells were seeded in 96-well plates (cell density: 1×10^3). After cell attachment (after 24 h), drugs were treated for 72 h. The viability of cells was assessed by using the CellTiter-Glo solution (#G3580; Promega, WI, USA), and absorbance was measured by SpectraMax device.

2.4. Immunoblot analysis

The cells were collected and lysed with RIPA buffer. The lysis buffer contained a phosphatase inhibitor (#524629; MERCK, Kenilworth, NJ, USA) and a protease inhibitor (#535140; MERCK). SDS-polyacrylamide gel electrophoresis was used to separate cell lysates. Afterward, gels were blotted onto PVDF membranes (#10600030; Amersham, Little Chalfont, UK). Membranes were incubated with primary antibodies overnight. In order to detect proteins, the SuperSignal™ Femto Substrate (#34095; Thermo Fisher Scientific) and the LAS-3000 detection system (Fujifilm, Tokyo, Japan) were employed. The following antibodies were purchased from Cell Signaling Technology (Danvers, MA, USA): p-EGFR (Y1068), EGFR, p-MET (Y1234/1235), MET, p-ERK (T202/Y204), ERK, p-AKT (S473), AKT, p-AURKB (T232), AURKB, p-His H3 (S10), His H3, Cleaved-Caspase3, BIM, p-BIM (S69), p-BIM (S87), pSTAT3 (T705), and STAT3. And b-Actin, GAPDH, C-MYC, BCL2, and OCT4 were purchased from Santa Cruz (Dallas, TX, USA).

2.5. Drug library screening

A total of 276 compounds from the Cambridge Cancer Compound Library (L2300, Selleckchem, Houston, TX, USA) were employed for screening purposes. Cells were seeded at a density of 1 × 103 cells/well in 384-well plates in quadruplicate. After overnight incubation,

the cells were treated with one drug at a 5-fold serial dilution for a total of six doses (50 μM to 16 nM). Cell viability was measured after 72 h of treatment using the CellTiter-Glo Luminescent cell viability assay kit (Promega, Madison, WI, USA) and an Infinite 200 Pro system (TECAN, Mannedorf, Switzerland). Each screening plate contained a dimethylsulfoxide-only vehicle control to calculate the relative cell viability and normalize the data. Dose-response curve fitting and area under the curve (AUC) values were assessed using GraphPad Prism 5.3 (GraphPad Software Inc., San Diego, CA, USA).

2.6. Colony formation assay

The cells were plated in 24-well plates at 2×10^3 cells/well and treated with the indicated drugs the next day. Medium change is performed every 3 days. After cell incubation for 14 days, cells were fixed with paraformaldehyde and stained with 0.1 % crystal violet solution.

2.7. Small interfering RNA

siRNA transfection was conducted using the Lipofectamine RNAiMAX Transfection Reagent (#13778150; Thermo Fisher Scientific) in accordance with the instructions provided by the manufacturer. AURKB and Scramble siRNA oligomers were transfected into cancer cell lines and analyzed after 48 h of incubation.

2.8. RNA sequencing and Validation

Total RNA was extracted using TRIzol (#15596026; Ambion, Austin, TX, USA) and a chloroform protocol. The Macrogen (Seoul, Korea) performed transcriptome library preparation and RNA sequencing. The libraries were prepared as poly(A)-RNA strands from 1 to 2 μg of total RNA using the TruSeq mRNA Kit (Illumina, San Diego, CA). The libraries were amplified via PCR, and after that, the libraries were sequenced using an Illumina HiSeq 2000 with 100bp paired-end reads per sample. The FastQC tool was employed to assess the quality of the raw reads. Following quality filtration with trimmomatic, the STAR 2 pass tool was utilized to align the RNA sequencing data to the GRCh38 of the human reference transcriptome. The Cancer Genome Atlas (TCGA) RNA-seq data, Mutation and Clinical annotation for Lung Adenocarcinoma were downloaded in mRNA-Seq expression (log2 (normalized RSEM+1)).

2.9. Gene set enrichment analysis

A differential expression analysis was conducted using the DESeq2 tool, and genes with a false discovery rate of <0.05 were subjected to Gene Set Enrichment Analysis (GSEA). GSEA was developed to determine differential expression levels of a predefined gene set in two different phenotypes, primarily using genomic and gene sequencing to detect biological

differences. We performed the GSEA (GSEA 4.2.3 version) using MSigDB C2 curated KEGG gene sets to compare parental with resistance cells. We identified pathways with a nominal p-value <0.05 as significant and chose them for further analysis. The GSEA software was downloaded at www.broadinstitute.org/gsea/ index.jsp. The RNA sequencing data from this study have been deposited in the Gene Expression Omnibus (GEO) under accession number GSE285996.

2.10. Quantitative real-time PCR

Total RNAs were extracted by using TRIzol (#15596026; Ambion, Austin, TX, USA) and cDNAs were synthesized from total RNA using Superscript II (#18064-022; Invitrogen, Carlsbad, CA, USA). Gene expression was investigated using RT-PCR on a Lightcycler®480 instrument(Roche, Basel, Switzerland). We ordered targeted gene primers from Cosmogenetech (Seoul, Korea). Experiments were run in triplicate. According to the manufacturer's protocol, reaction mixtures were prepared with Sensi FAST SYBR No-ROX mix (#BIO-98005; Bioline, London, UK). The expression of each gene was analyzed and quantified using ΔΔCq method normalized by GAPDH gene expression (Table 1).

Table 1. Sequences of the RT-qPCR primers.

Target gene	Sequence (5'-3')	Target gene	Sequence (5'-3')
AURKB	forward: GGAGTGCTTTGCTATGAGCTGC reverse: GAGCAGTTTGGAGATGAGGTCC	*PUMA*	forward: ACGACCTCAACGCACAGTACGA reverse: CCTAATTGGGCTCCATCTCGGG
STAT3	forward: CTTTGAGACCGAGGTGTATCACC reverse: GGTCAGCATGTTGTACCACAGG	*BAD*	forward: CCAACCTCTGGGCAGCACAGC reverse: TTTGCCGCATCTGCGTTGCTGT
CCNB1	forward: GACCTGTGTCAGGCTTTCTCTG reverse: GGTATTTTGGTCTGACTGCTTGC	*BID*	forward: TGGGACACTGTGAACCAGGAGT reverse: GAGGAAGCCAAACACCAGTAG
CCND1	forward: TCTGGCATTTTGGAGAGGAAGTG reverse: TCTACACCGACAACTCCATCCG	*BIM*	forward: CAAGAGTTGCGGCGTATTGGAG reverse: ACACCAGGCGGACAATGTAACG
BCL2	forward: ATCGCCCTGTGGATGACTGAGT reverse: GCCAGGAGAAATCAAACAGAGGC	*NOXA*	forward: CTCGATGCAGAGACAGAGGTCC reverse: AGGAGCCTGTTTGCCAACTTGC
BCLXL	forward: GCCACTTACCTGAATGACCACC reverse: AACCAGCGGTTGAAGCGTTCCT	*BAX*	forward: TCAGGATGCGTCCACCAAGAAG reverse: TGTGTCCACGGCGGCAATCATC
MCL1	forward: CCAAGAAAGCTGCATCGAACCAT reverse: CAGCACATTCCTGATGCCACCT	*BAK*	forward: TTACCGCCATCAGCAGGAACAG reverse: GGAACTCTGAGTCATAGCGTCG
C-MYC	forward: CCTGGTGCTCCATGAGGAGAC reverse: CAGACTCTGACCTTTTGCCAGG	*GAPDH*	forward: GTCTCCTCTGACTTCAACAGCG reverse: ACCACCCTGTTGCTGTAGCCAA
SOX2	forward: GCTACAGCATGATGCAGGACCA reverse: TCTGCGAGCTGGTCATGGAGTT		
OCT4	forward: CCTGAAGCAGAAGAGGATCACC reverse: AAAGCGGCAGATGGTCGTTTGG		

2.11. Cell cycle and Flow cytometry

To detect apoptosis, we used the Annexin-V FITC apoptosis detection kit (#556547; BD Biosciences, San Diego, CA, USA). The cells were grown in 100 mm plates and treated with the indicated drugs for 48 h. Following the administration of the drugs, the cells were harvested with trypsin, washed with phosphate-buffered saline PBS, and suspended with Annexin-V binding buffer. Following suspension in binding buffer, cells were subjected to a double staining procedure using an apoptosis detection kit. The cells were incubated at room temperature in the dark for 30 min and subsequently analyzed by flow cytometry. The cell cycle was detected using FxCycleTMPI/RNase Staining Solution (#F10797; Invitrogen, Carlsbad, CA, USA). The samples were prepared in accordance with the manufacturer's instructions.

2.12. Mouse xenograft

Approval for the conduct of mouse xenograft studies has been granted by the National Cancer Center (accession number IACUC-A202310-1748-01).We used 6-week-old N2G (NOD-Prkdcnullll2rgnull) male mice (Gemcro, Korea). The mice were randomly divided into four groups according to weight (average 23 g–24 g). Prior to the injection of cancer cells, the mice underwent an adaptation period of 1 week. In order to facilitate the adaptation of the mice,

we provided them with comfortable bedding. A total of 2 × 106 cells were injected into the mice, with 50 % Matrigel used as a vehicle. The tumor volume was then measured using a caliper on a weekly basis. Mice were given intraperitonealinjections of the PHA665752 at a dosage of 25 mg/kg/day (n = 7), barasertib at a dosage of 50 mg/kg/day (n = 7), and combination treatment of PHA665752 and barasertib (n = 7) once every 2 days for 3 weeks in each volume of 100 μl; another 7 control mice were given vehicle (8 % dimethyl sulfoxide, 50 % polyethylene glycol, 5 % tween 80, and 37 % ddH2O). After 3 weeks of treatment, euthanasia was induced by injecting continuous CO2 flow into the cage. Upon confirmation that the mouse was no longer breathing, the injection of carbon dioxide was terminated. The xenograft tumors were resected and fixed in 4 % paraformaldehyde for immunohistochemistry. All animal experimentswere conducted in accordance with the guidelines of our institutional animal care and use committee and in compliance with all relevant ethical regulations.

2.13. Immunohistochemistry

All mouse xenograft tumors were prepared in formalin-fixed paraffin-embedded blocks and cut into two consecutive sections (3 μm). One tumor section was stained with a polyclonal Ki-67 antibody (AB15580; Abcam), while the other was used for hematoxylin and eosin (H&E) to determine tumor cell morphology. Patient tumors were fixed with formalin and embedded in paraffin. Following the preparation of sections on glass slides (3 μm),

immunostaining was conducted at the Laboratory Animal Research Facility of the National Cancer Center using an AURKB antibody (LS-B1451; LSBio). Quantitative analysis was conducted using the Vectra Polaris Imaging System and Inform software (Akoya Biosciences, USA).

2.14. Droplet digital PCR

ddPCR was conducted by using a QX200 system (Bio-Rad, Hercules, CA, USA). The TaqMan Probe mix solutions for PCR reaction were prepared according to the manufacturer's protocol (*MET* CNV FAM; #10031240, HEX; #10031243). After PCR was complete, the oil droplet was read by a droplet reader to detect TaqMan Probe fluorescence in individual droplets using.

2.15. Immunofluorescence staining

Cells were seeded in chamber slides and, after 24 h, washed with PBS three times for 5 min. By using 4 % formaldehyde, cells were fixed at RT for 10 min and blocked with immunofluorescence blocking buffer for 1 h (12411S; Cell signaling). After that, cells were incubated with 1' antibody at 4 °C. 24 h later, cells were washed with PBS and incubated with a 2' antibody for 1 h. After PBS wash, cells were mounted with ProLong Gold buffer (8961S;

Cell signaling).

2.16. Cell migration assay

Cells were seeded onto a trans-well chamber (Costar Co., MA) containing 8 μm pore size polycarbonate membranes. Cells were harvested and resuspended in culture media without 10 % FBS. Cells were seeded in the upper chamber of a 12-well plate (2×10^5 cells/well). The lower chambers were filled with 0.5 mL of RPMI plus 10 % FBS. After incubation of 72 h, the membrane-contained chamber was fixed with 4 % formaldehyde and stained with crystal violet solution (0.1 %). After that, the upper membrane of the inner chambers was wiped with a cotton swab.

2.17. Ethics approval and Consent to participate

Two patients with advanced NSCLC undergoing treatment at the National Cancer Center participated with written informed consent in the study for the collection of tissue and translational research was approved by the National Cancer Center Hospital Institutional Review Board (NCC2016-0208) (Goyang, Korea). Tumor biopsies were performed on each patient before and after treatment with MET inhibitors.

2.18. Statistical analysis

At least all experiment was conducted three times, and all results are shown as the mean ± SEM. Statistical analysis was conducted by using a t-test (two-sample). p-values ≤ 0.05 were considered significant (*$p < 0.05$, **$p < 0.01$, ***$p < 0.001$; ns, not significant).

3. RESULTS

3.1. AURKB activation in MET-TKI acquired resistance cell line

The non-small cell lung cancer cell line harboring *MET*-amplification (H1993) was used in this research, and the acquired resistance cell line (H1993 PR-S2) was established by chronic exposure to MET-TKI **(Fig 4A)**. The cell viability was conducted to confirm the complete PHA665752 resistance of the H1993 PR-S2 cells in contrast to the H1993 cells **(Fig 4B-C).** In addition, the H1993 PR-S2 cells showed resistance to Type I MET inhibitor (capmatinib) and Type II MET inhibitors (cabozantinib and crizotinib) **(Figure 4B-C)**.

To ascertain the original characteristics of *MET*-amplified cancer cells, H1993, the *MET* gene copy number variation (CNV), and the H1993 PR-S2 cells proliferation rate were investigated. The *MET* CNV rate of the H1993 PR-S2 cells was similar to that of the H1993 cells (*MET* CNV; H1993 = 18.7, H1993 PR-S2 = 20.8) **(Figure 5A)**, whereas the H1993 PR-S2 cells proliferation rate was lower than that of the H1993 cells **(Figure 4D)**. Next, to determine the genomic variations between the H1993 cells and the H1993 PR-S2 cells, the whole exome sequencing analysis was conducted. However, in the H1993 PR-S2 cells, no secondary point mutations were detected in the *MET* kinase domain **(Fig 5C)** or other molecular alterations, including *KRAS*, *EGFR* and *HER3*[22], which had previously been identified as resistance mechanisms in other studies **(Table 2)**. In the next step, we investigated whether the basal

expression levels of the MET and EGFR proteins, as well as downstream kinase, were altered in the H1993 PR-S2 cells. In immunoblot analysis, the protein expressions of total MET and p-MET were fully reduced in the H1993 PR-S2 cells compared to the H1993 cells. However, these two cell lines did not differ in the protein levels of ERK, which is downstream of MET. Furthermore, the EGFR/AKT pathway, widely recognized as a bypass mechanism for MET-TKI[29], was not upregulated in the H1993 PR-S2 cells **(Fig 4E)**. The H1993 PR-S2 cells also showed resistance to EGFR-TKI (Gefitinib), PHA665752, and combination treatment **(Fig 4F)**. Consequently, the EGFR pathway was postulated not to be an alternative acquired resistance mechanism of the H1993 PR-S2 cells. These results led to the hypothesis that the H1993 PR-S2 cells employ alternative molecular mechanisms to develop resistance against MET-TKI, PHA665752, independent of the EGFR or MET receptor-mediated pathways.

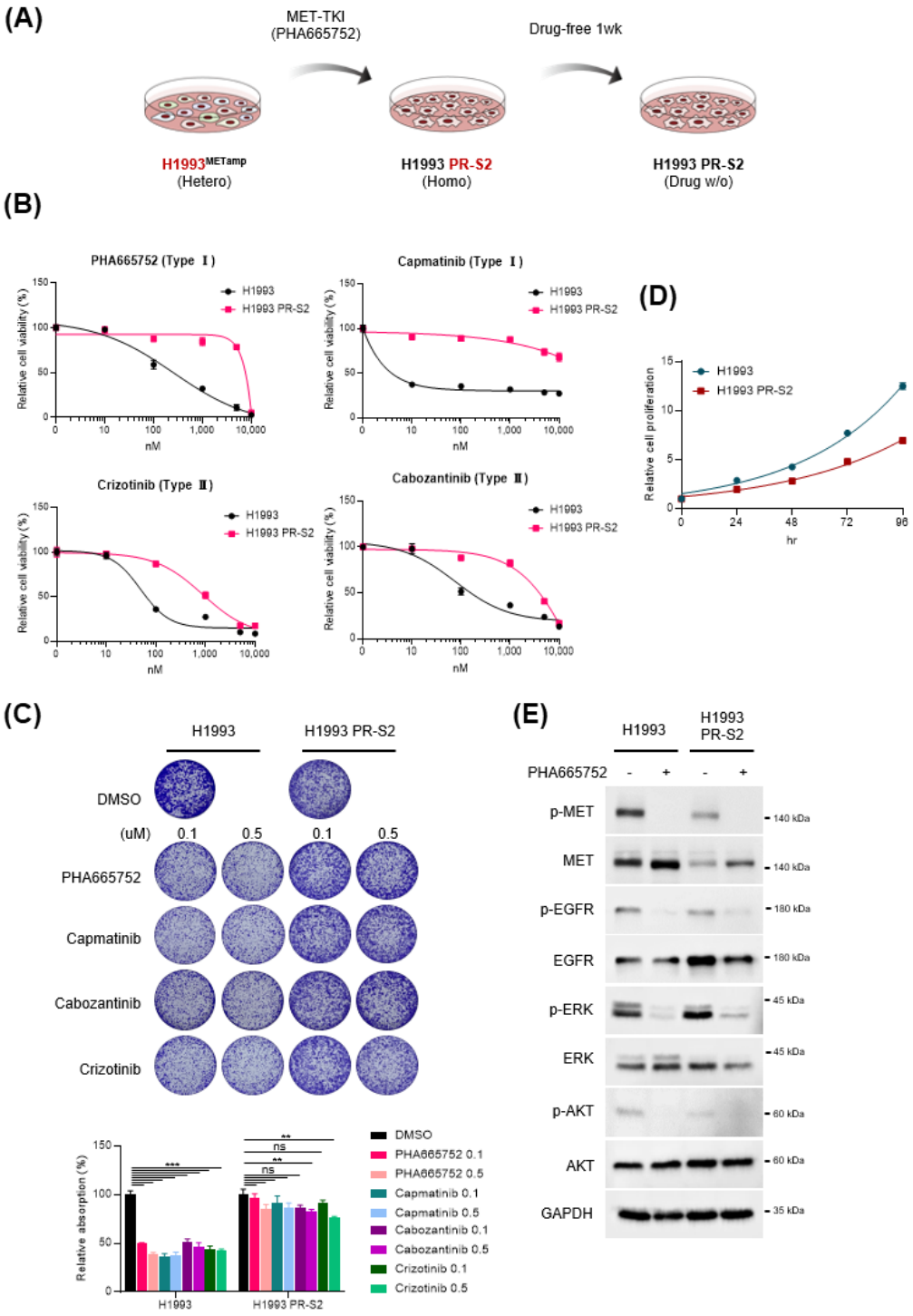

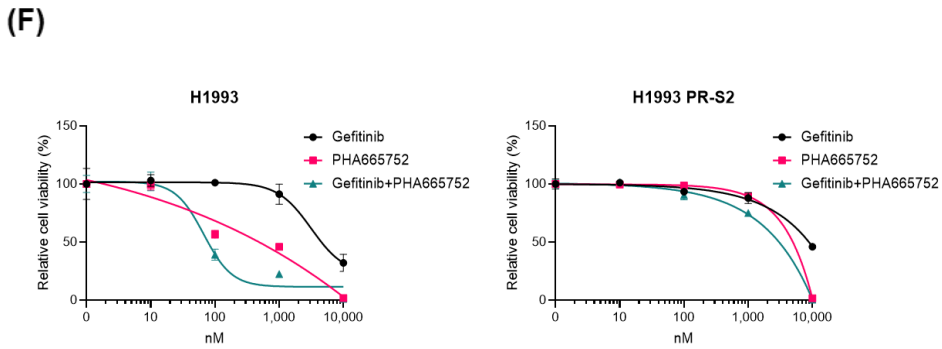

Fig 4. Generation of MET-TKI acquired resistance cell line. (A) A diagrammatic summary of the generation of the drug-resistant cell line up to 1 μM MET-TKI (PHA665752). (B) Mean relative viability of the H1993 and H1993 PR-S2 cells against PHA665752, capmatinib, cabozantinib, and crizotinib treatment. (C) Crystal violet staining after 8 days of indicated drug treatment. The bar graph illustrates the relative absorption of destaining of crystal violet. (D) The relative proliferation rate of the H1993 and H1993 PR-S2 cells. (E) Immunoblot analysis of the H1993 and H1993 PR-S2 cells with or without MET-TKI. (F) Mean relative viability of the H1993 and H1993 PR-S2 cells against gefitinib, PHA665752, and combination treatment. The standard error of the mean (SEM) is indicated by the error bars (n = 3). Statistical analysis was performed using a two-sample t-test. ns, not significant; **p< 0.01; ***p< 0.001. Abbreviation: w/o, without.

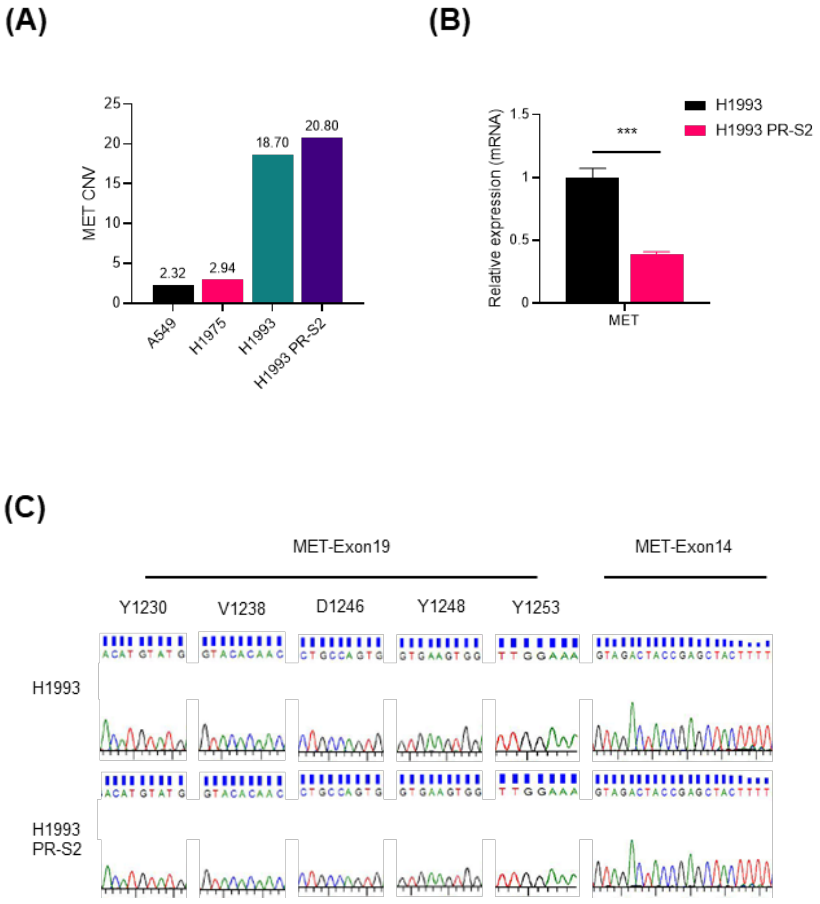

Fig 5. Mutation of the *MET* gene in MET-TKI acquired resistance cell line. (A) Copy number variation of *MET*. (B) mRNA expression of *MET*. (C) Direct sequencing analysis of the exon 14 and exon 19 mutations of *MET*. The standard error of the mean (SEM) is indicated by the error bars (n = 3). Statistical analysis was performed using a two-sample t-test. ***p< 0.001.

Table 2. The whole exome sequencing mutation calling list of the H1993 PR-S2 cell line compared to the H1993 cell line.

H1993 PR-S2 mutations
DNAJC6,SUPT6H,FLOT2,CPT1C,ADAM20,ANAPC1,PTPRR,FAM73B,FCAMR,RNF43,CNGB1,SEC31B,TVP23A,SZT2,SLC2A9,ITGA11,HOMER3,URGCP,TAL1,HOXA1,SLC1A2,SGK1,DNAJC16,KCNQ4,ELN,PGS1,SORL1,NLRP9,ASIC1,POU3F4,CDC42BPB,CLDN11,TSPAN31,FAH,LRP1B,TCHH,IKBKE,SLC7A8,AP3D1,TPTE2,ZNF3,NEB,TNK2,KANSL3,FBXO17,NRAP,SLC1A7,KAT6B,WFDC2,FAM208B,SLC26A4,HOXA3,C1orf68,THBS4,KCNJ14,SLCO6A1,FXR1,FAR2,MUC3A,C2CD2,NMRAL1,RUSC1,SMCHD1,RTTN,ATM

To discover potential strategies to overcome MET-TKI acquired resistance, a high-throughput drug screening assay was conducted with a druggable inhibitor library of 276 compounds. The 10 compounds were rearranged according to values of area under the curve, which means higher sensitivity against the H1993 PR-S2 cells than the parental cell line **(Fig 6A-B)**. Interestingly, the pan-AURK inhibitors (VX-680 and SNS-314) showed high sensitivity in the H1993 PR-S2 cells **(Fig 6A-B)**.

Cell viability assays were performed using an AURK pan inhibitor (VX680), an AURKB inhibitor (barasertib), and an AURKA inhibitor (MLN8237, AT9283) to determine which of the three AURK molecules (AURKA, AURKB, AURKC) is the major AURK molecule. Among the types of aurora kinase inhibitors, the AURKB inhibitor, barasertib, showed the highest sensitivity to the H1993 PR-S2 cells than the parental cells **(Fig 6C)**.

(A)

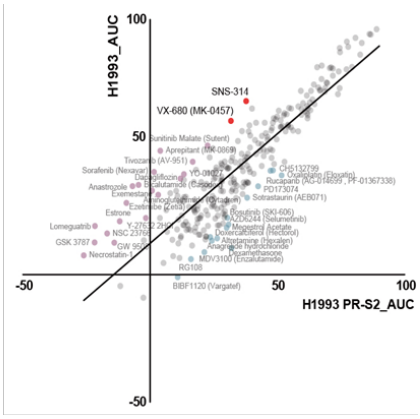

(B)

	Inhibitor	Target	AUC [H1993-(PR-S2)]
1	GSK3787	PPAR	33.53
2	NSC23766	Rac	31.84
3	Ezetimibe	Cholesterol	29.79
4	Cytadren	Aromatase	25.84
5	**SNS-314**	**Aurora Kinase**	**25.44**
6	Sutent	VEGFR	24.4
7	**MK0457**	**Aurora Kinase**	**24.21**
8	YO-01027	Gamma secretase	23.27
9	Dafaglifozin	SGLT	23.03
10	Y-27632-2Hcl	ROCK	22.26

(C)

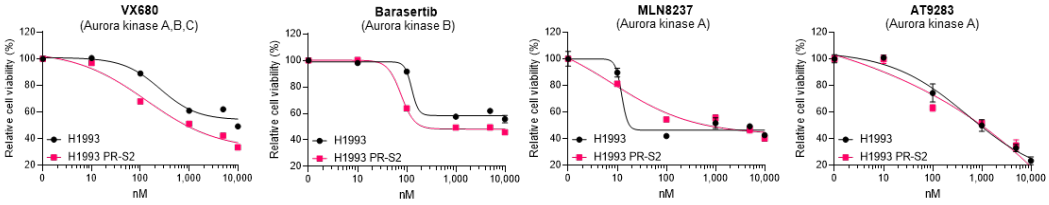

Fig 6. The high throughput inhibitor screening analysis in the H1993 and H1993 PR-S2 cells.

(A) The calculation result of the area under the curve from high throughput inhibitor screening (HTS) analysis of the H1993 PR-S2 cells compared to the H1993 cells. (B) Comparison of area under the curve (AUC) values and rearrangement of 10 high-sensitivity compounds in the H1993 PR-S2 cells. (C) Mean relative cell viability of the H1993 and H1993 PR-S2 cells against various AURK inhibitors. The standard error of the mean (SEM) is indicated by the error bars (n = 3).

To validate the effect of the AURKB inhibitor, clonogenic assays were conducted to evaluate the extent of growth inhibition against PHA665752 and barasertib. The clonogenic assays demonstrated that barasertib inhibited the cell growth of the H1993 PR-S2 cells significantly. In contrast, barasertib had no effect on the H1993 cells, while PHA665752 inhibited parental cell proliferation **(Fig 7A)**. These data demonstrated that the inhibition of AURKB was sufficient for the growth inhibition of the H1993 PR-S2 cells. Interestingly, the knockdown of AURKB in the H1993 PR-S2 cells demonstrated increased sensitivity to PHA665752. The parental cells remain sensitive to PHA665752, irrespective of the knockdown of the *AURKB* gene **(Fig 7B-C)**.

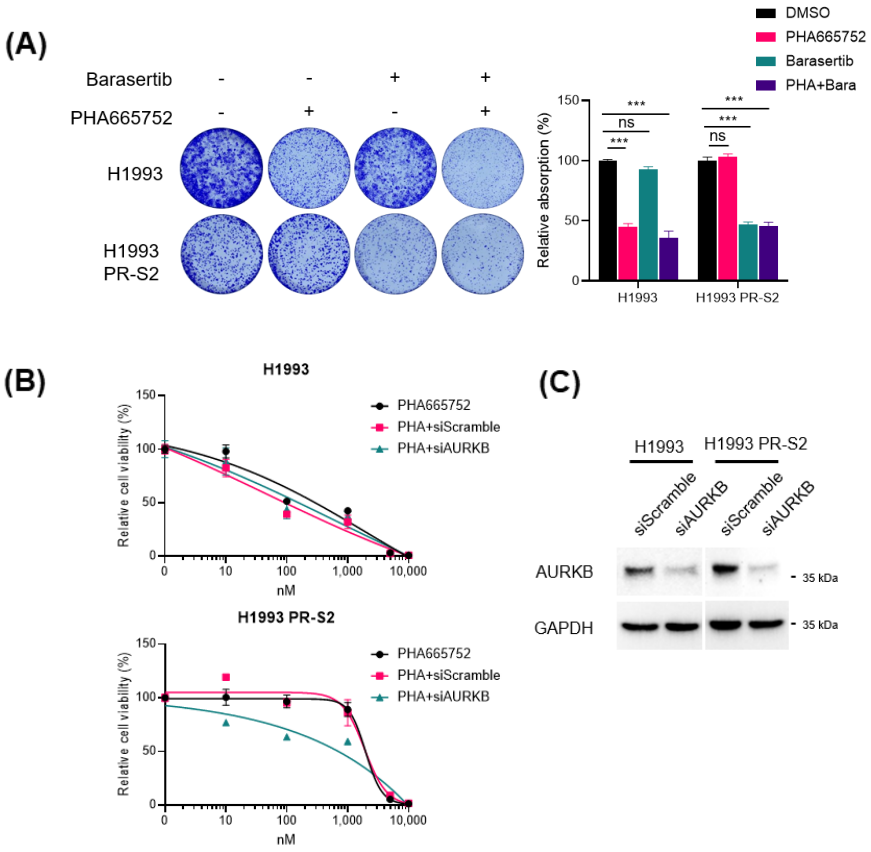

Fig 7. Growth inhibition effect of decreased AURKB expression. (A) The results of the crystal violet staining procedure were conducted after 8 days of treatment with dimethyl sulfoxide or the indicated drugs. The bar graph illustrates the relative absorption of destaining of crystal violet. (B) Mean relative viability of the H1993 and H1993 PR-S2 cells against PHA665752 with or without AURKB knockdown. (C) Protein expression of AURKB after treatment of scramble and siAURKB in the H1993 and H1993 PR-S2 cells. The standard error of the mean (SEM) is indicated by the error bars (n = 3). Statistical analysis was performed using a two-sample t-test. ns, not significant; ***p< 0.001.

The subsequent step was to find the differentiation of AURKB expression between the H1993 and H1993 PR-S2 cells. The protein expression of total AURKB and phosphorylated AURKB was elevated in the H1993 PR-S2 cells, in contrast to a lack of corresponding changes in mRNA expression **(Fig 8A-B)**. In a previous study, histone H3 activation (p-His H3 S10) was identified as a downstream target of AURKB[30], and its upregulation was reported to be associated with gefitinib resistance in PC9 cells[31]. However, western blot data showed that the mechanism of MET-TKI resistance did not rely on His H3-related pathways because protein expression of total His H3 and p-His H3 was not increased in the H1993 PR-S2 cells **(Fig 8B)**. Regardless of His H3 activation, the H1993 PR-S2 cells were more sensitive to the downregulation of AURKB protein expression at lower concentrations of barasertib compared to the H1993 cells **(Fig 8C)**. However, the kinetics of AURKB protein degradation in the H1993 PR-S2 cells were similar to that observed in the H1993 cells. **(Fig 8D)**. From these part, experimental findings demonstrated that the upregulated AURKB expression is essential for maintaining the MET-TKI acquired resistance, and inhibition of AURKB was sufficient to inhibit the growth of the H1993 PR-S2 cells.

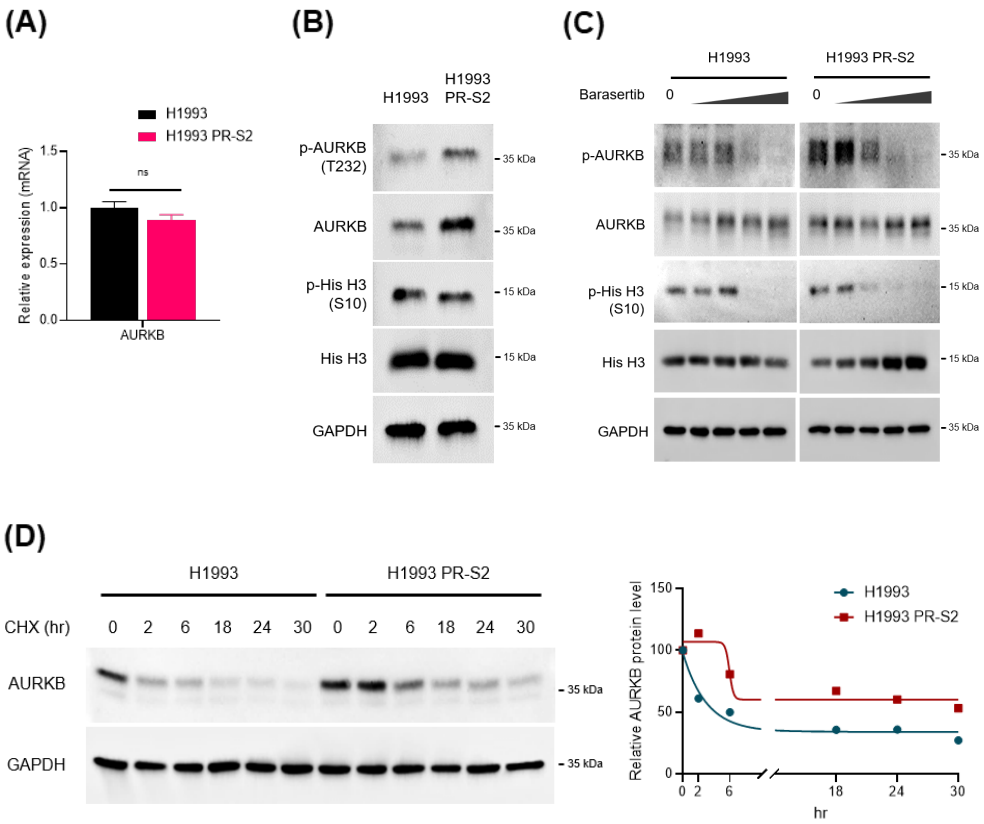

Fig 8. Comparison of AURKB expression in the H1993 and H1993 PR-S2 cells. (A) mRNA expressions of *AURKB* in the H1993 and H1993 PR-S2 cells. (B) Immunoblot analysis of proteins and phosphor proteins of AURKB and Histone H3 in lysates of the H1993 and H1993 PR-S2 cells. (C) Immunoblot analysis of AURKB and His H3 proteins and phosphorylated proteins after 24 h dose-dependent treatment of AURKB inhibitor (barasertib) (0.01, 0.1, 1, 10 μM). (D) AURKB protein stability after treatment with 10 μg/ml cycloheximide for the indicated treatment time in the H1993 and H1993 PR-S2 cells. The line graph represents the relative AURKB band intensity

of the western blot. The standard error of the mean (SEM) is indicated by the error bars (n = 3). Statistical analysis was performed using a two-sample t-test. ns, not significant.

3.2. Stimulation of STAT3-BCL2 axis by AURKB

Next, to know what pathway is mediated by AURKB, gene set enrichment analysis (GSEA) was performed to explore the significant differences in gene expression between the parental and resistant cells. GSEA data analysis revealed that downstream targets of STAT3 were significantly upregulated in the H1993 PR-S2 cells compared to the H1993 cells **(Fig 9A)**. This result was corroborated by the observation of increased p-STAT3 protein in the H1993 PR-S2 cells **(Fig 9B)**. The immunoblot analysis proceeded to examine the levels of the JAK family of proteins, which are known to be major upstream regulators of STAT3. Unexpectedly, in the H1993 PR-S2 cells, there was a notable decrease in the JAK family protein expression levels compared to the parental cell line **(Fig 10)**. Consequently, this results indicated that another kinase might phosphorylate STAT3 independently of several RTKs, including EGFR, MET, and JAK.

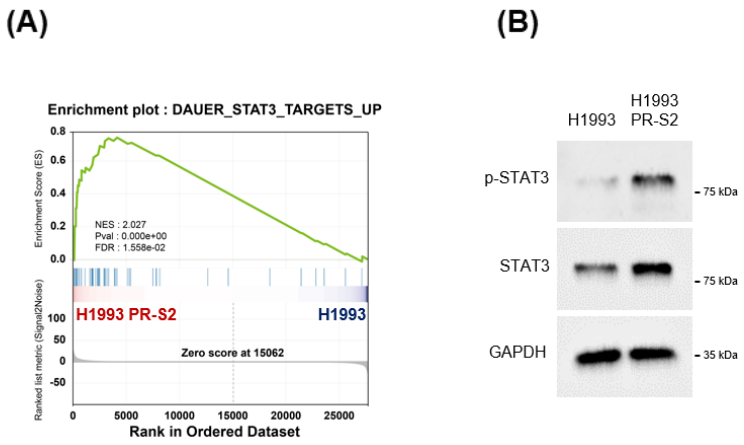

Fig 9. Elevated STAT3 expression in the H1993 PR-S2 cells. (A) Gene set enrichment (GSEA) data of upregulated STAT3 target genes in the H1993 PR-S2 cells. (B) Protein expressions of p-STAT3, STAT3, and GAPDH.

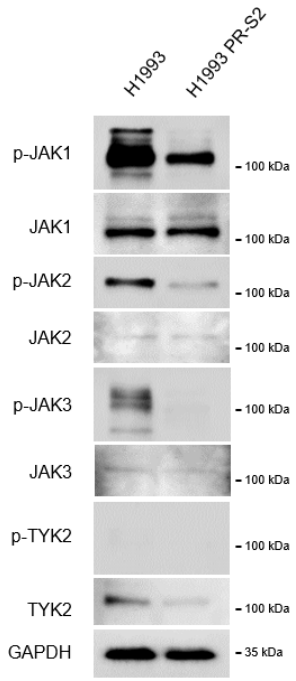

Fig 10. JAK family protein expression in the H1993 and H1993 PR-S2 cells. JAK family and GAPDH protein expressions in parental and MET-TKI acquired resistance cell lines.

Given that AURKB is known to be a serine/threonine kinase, the objective was to determine whether AURKB regulation could influence STAT3 phosphorylation. Treatment with the AURKB inhibitor resulted in a reduction in p-STAT3 expression in the H1993 PR-S2 cells without affecting p-AKT and p-ERK levels **(Fig 11A-B)**. The expression of cleaved caspase-3, the apoptotic cell death marker, was increased in the barasertib-treated H1993 PR-S2 cells, while the expression of p-STAT3 was decreased **(Fig 11A)**. The reduction of AURKB expression by siRNA treatment induced a significant reduction of p-STAT3 expression in the H1993 PR-S2 cells **(Fig 11C)**. Conversely, an elevated expression of pSTAT3 was observed in the AURKB-overexpressed H1993 stable cell line (H1993_AURKB-GFP), which had been established through the artificial infection of a virus **(Fig 11D)**. The binding of AURKB and STAT3 does not occur in both cell lines **(Fig 11E)**. Furthermore, we sought to determine whether long-lived AURKB affects STAT3 protein stability. Treatment with the proteasome inhibitor MG132 led to the accumulation of pSTAT3 protein in the H1993_AURKB-GFP cells **(Fig 11F)**. These findings indicated that AURKB could regulate STAT3 activation independently of the MET activation pathway in the H1993 PR-S2 cells.

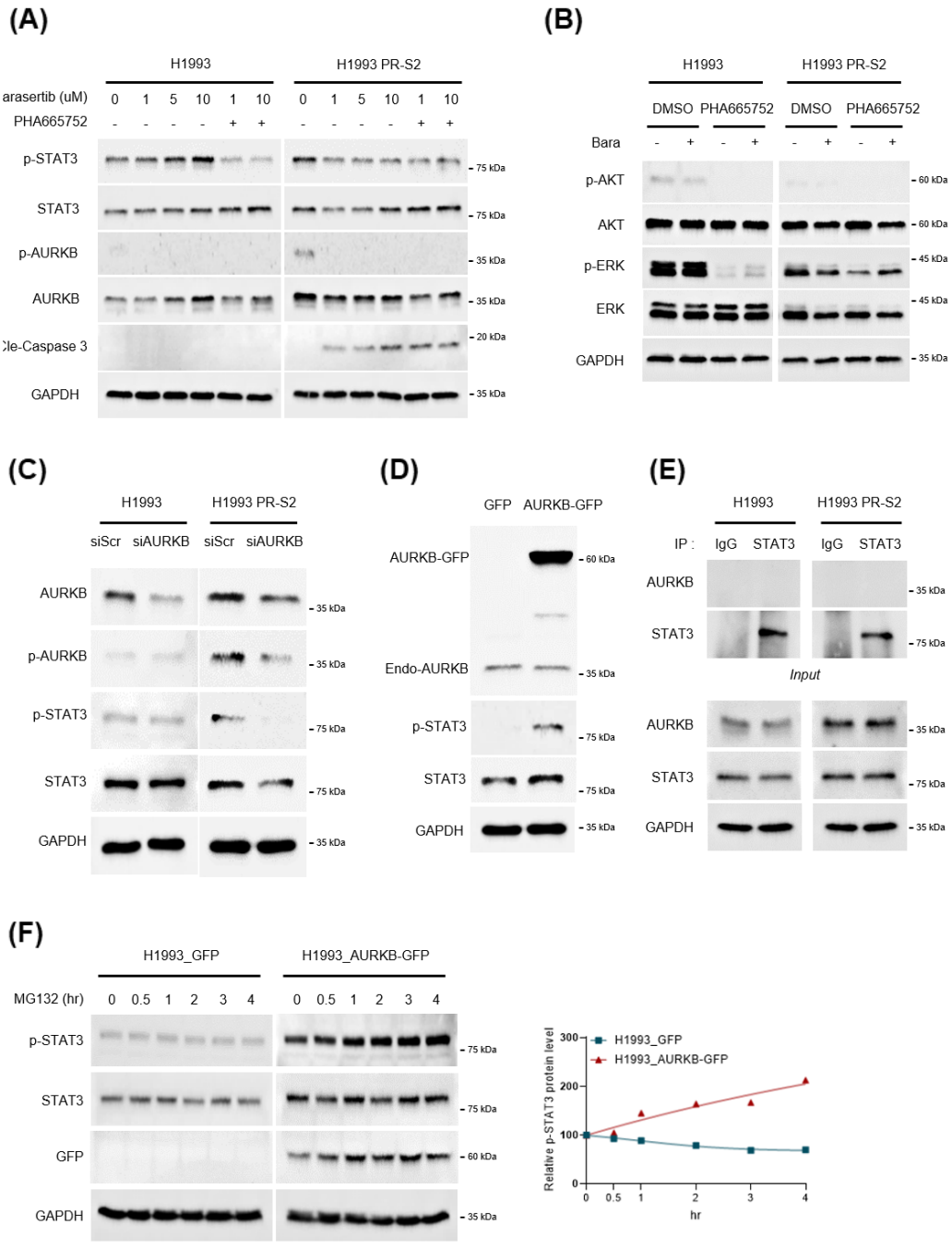

Fig 11. Positive regulation of p-STAT3 expression by AURKB. (A) Protein expressions of p-STAT3, STAT3, p-AURKB, AURKB, and GAPDH after barasertib single or PHA665752 combination treatment of indicated drug concentration for 48 h. (B) Expression of total and active forms of AKT and ERK proteins. (C) Immunoblot analysis of the H1993 and H1993 PR-S2 cells transfected with scramble and siAURKB for 48 h. (D) and (E) The indicated protein expressions of the GFP and AURKB-GFP virus-infected H1993 stable cell lines and MG132 treatment for the indicated treatment time. The line graph represents the protein stability of p-STAT3. (F) Immunoprecipitation analysis between STAT3 and AURKB. The standard error of the mean (SEM) is indicated by the error bars (n = 3).

To elucidate the downstream target of activated STAT3 in the H1993 PR-S2 cells, we conducted an investigation into the mRNA changes of downstream targets of STAT3. Among the several STAT3-related downstream target genes, the mRNA and protein levels of the antiapoptotic protein BCL2 were found to be significantly increased in the H1993 PR-S2 cells **(Fig 12A-B)**. The STAT3 knockdown notably reduced this upregulated BCL2 expression, both mRNA and protein, without affecting the mRNA levels of other STAT3 target genes **(Fig 12C)**. Although knockdown of STAT3 in H1993 PR-S2 cells did not improve MET-TKI sensitivity **(Fig 13A-B)**, interestingly, AURKB inhibition resulted in a reduction of BCL2 mRNA and protein levels, accompanied by an increase in the expression of cleaved-caspase3, a marker of apoptotic cell death **(Fig 13C-D)**. Thus, these findings indicated that AURKB inhibition regulates the anti-apoptotic process by suppressing the STAT3-BCL2 axis to overcome PHA665752 resistance.

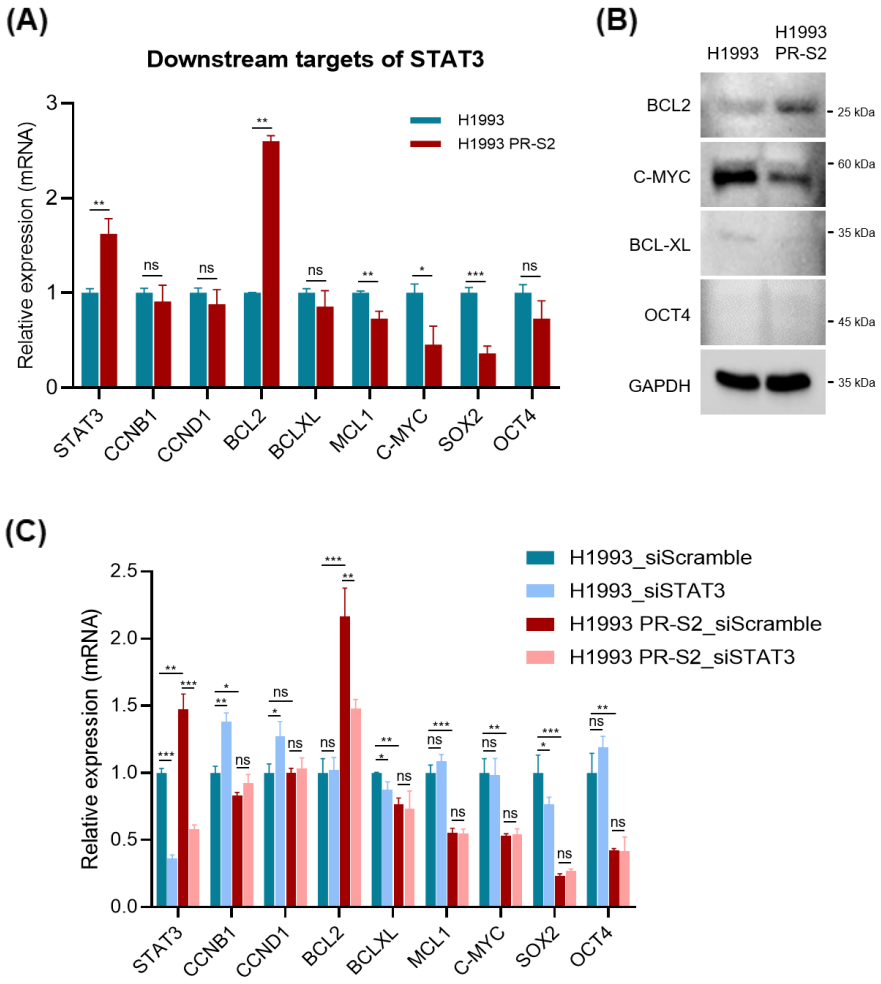

Fig 12. Increased *BCL2* mRNA expression downregulated by STAT3 knockdown. (A) and (B) RT-qPCR and western blot analysis of the expression levels of STAT3 downstream targets. (C) mRNA expression of STAT3 target genes in the scramble or siSTAT3 transfected H1993 and H1993 PR-S2 cells. The standard error of the mean (SEM) is indicated by the error bars. The standard error of the mean (SEM) is indicated by the error bars (n = 3). Statistical analysis was performed using a two-sample t-test. ns, not significant; *p< 0.05; **p< 0.01; ***p< 0.001.

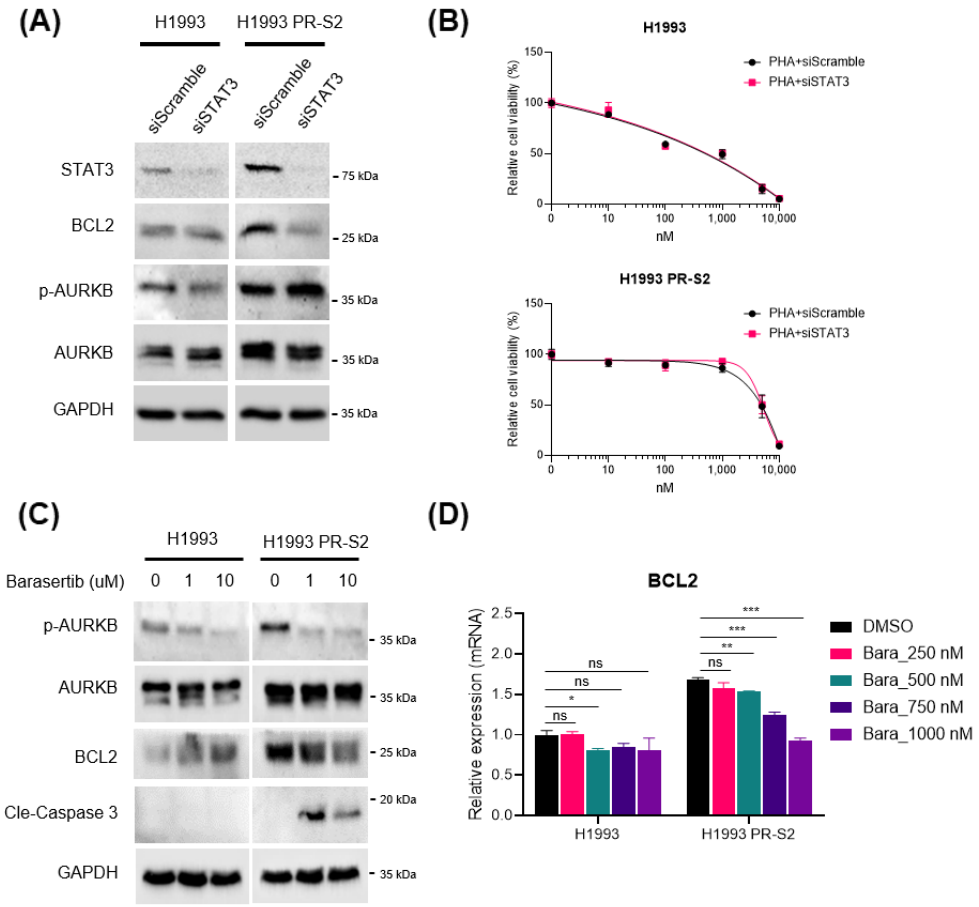

Fig 13. Reduced mRNA expression of *BCL2* and induced cell death by AURKB inhibitor. (A) Immunoblot analysis of the H1993 and H1993 PR-S2 cells transfected with scramble and siSTAT3 for 48 h. (B) (C)Protein expression of cleavage-caspase3 and BCL2 after treatment with barasertib for 48 h. (D) mRNA expression levels of BCL2 after treatment with barasertib at concentrations ranging from 250 to 1000 nM. The standard error of the mean (SEM) is indicated by the error bars (n = 3). Statistical analysis was performed using a two-sample t-test. ns, not significant; *p< 0.05; **p< 0.01; ***p< 0.001. Abbreviation: Bara, barasertib.

3.3. Induced apoptotic cell death by AURKB inhibition

The mechanism underlying barasertib-induced apoptotic cell death of the MET-TKI resistance cell line was investigated by examining mRNA expressions of apoptosis-related genes. Among the numerous apoptosis-related genes, the pro-apoptosis gene BIM was found to be significantly downregulated in the H1993 PR-S2 cells **(Fig 14)**. Previous study reported that proapoptotic protein BIM is downstream of ERK, and ERK and AURKB can stabilize and degradate BIM through each phosphorylation (S69 and S87)[32]. In the H1993 PR-S2 cells, we sought to ascertain whether AURKB inhibition altered BIM protein expression. The data demonstrated that PHA665752 reduced p-ERK protein levels and induced BIM_{EL} accumulation in the H1993 cells but not in the H1993 PR-S2 cells. Conversely, barasertib treatment resulted in BIM_{EL} accumulation in the H1993 PR-S2 cells without affecting p-ERK protein expression **(Fig 15A)**. Notably, the inhibition of AURKB resulted in a decreased expression of p-BIM (S87) in the H1993 PR-S2 cells but not in the parental cell line **(Fig 15B)**. These results indicated that AURKB inhibition is sufficient to induce BIM accumulation in the H1993 PR-S2 cells.

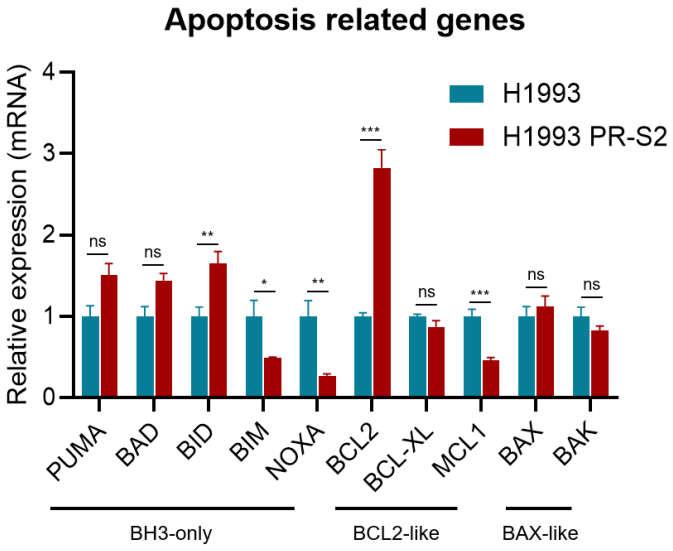

Fig 14. The mRNA expression of apoptosis-related genes in the H1993 and H1993 PR-S2 cells.

The RT-qPCR measured the expression of apoptosis-related genes in the H1993 and H1993 PR-S2 cells. The standard error of the mean (SEM) is indicated by the error bars (n = 3). Statistical analysis was performed using a two-sample t-test. ns, not significant; *p< 0.05; **p< 0.01; ***p< 0.001.

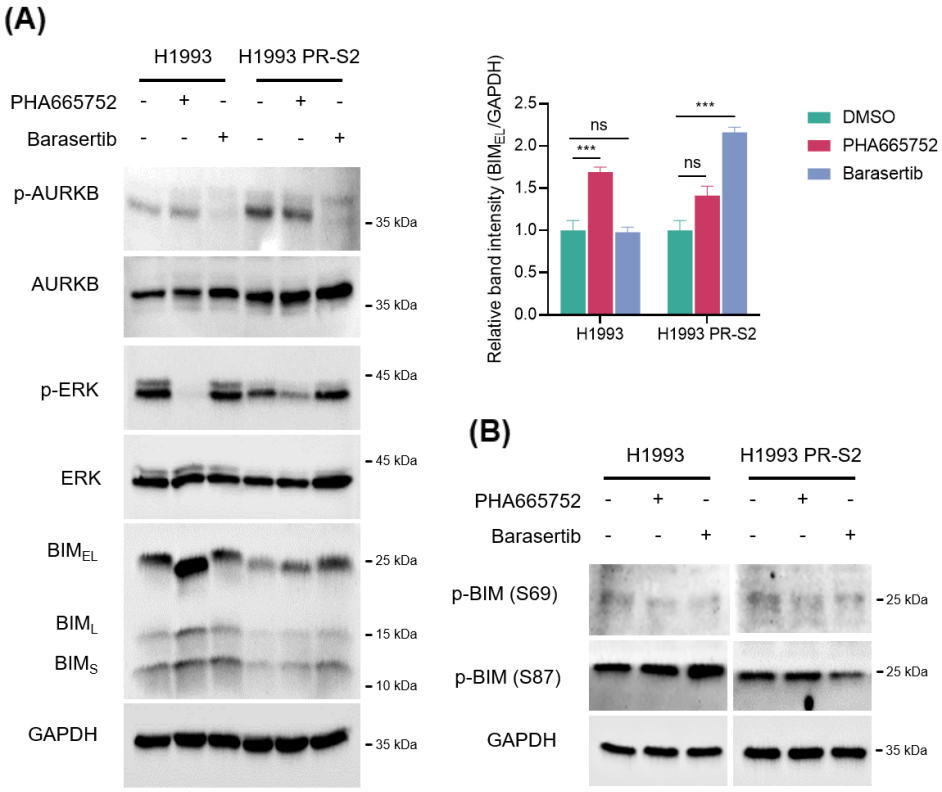

Fig 15. BIM_{EL} accumulation after inhibition of AURKB. (A) Western blot analysis in the H1993 and H1993 PR-S2 cells after treatment MET inhibitor or AURKB inhibitor (each 1 μM) for 48 h. The bar graph represents the band intensity of BIM_{EL}. **(B)** The activated form expression of BIM protein (S87) in the H1993 and H1993 PR-S2 cells. The standard error of the mean (SEM) is indicated by the error bars (n = 3). Statistical analysis was performed using a two-sample t-test. ns, not significant; ***p< 0.001.

As AURKB is known to be a cell cycle-related molecule, it has been reported that AURKB inhibition induces the formation of polyploid giant cells, G2/M cell cycle arrest, and apoptotic cell death[33]. The impact of barasertib was examined on the cell cycle of both H1993 cells and H1993 PR-S2 cells. The cell cycle change was investigated in live cells treated with 100, 250, and 500 nM barasertib. While barasertib had a minimal effect on the H1993 cells, it induced G2/M cell cycle arrest at lower inhibitor concentrations in the H1993 PR-S2 cells **(Fig 16)**. Following the induction of G2/M cell cycle arrest, the percentage of early apoptotic cells significantly increased in the barasertib-treated H1993 PR-S2 cells compared to the parental cell line, as demonstrated by Annexin-V-FITC staining of flow cytometry (FACs) analysis **(Fig 17A)**. Furthermore, the formation of polyploid giant cells was observed to increase in both the H1993 cells and the H1993 PR-S2 cells **(data not shown)**, while the cleaved caspase 3 expression was found to be significantly elevated in the H1993 PR-S2 cells **(Fig 17B)**. These findings indicate that AURKB inhibition is sufficient to induce BIM_{EL} accumulation and apoptotic cell death in the PHA665752-resistant cell line.

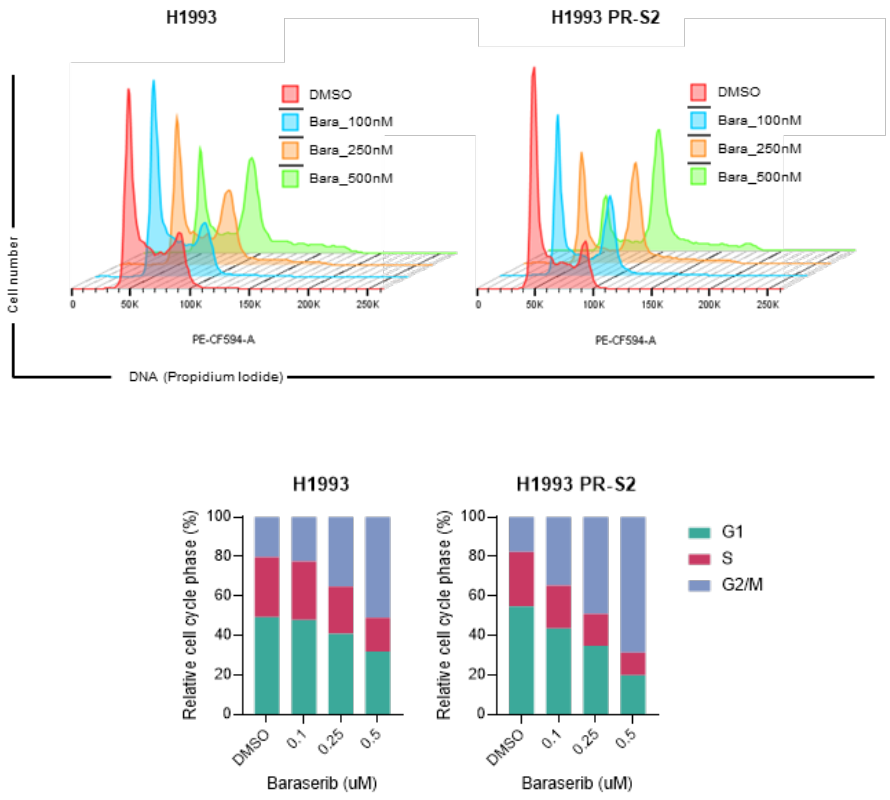

Fig 16. The G2/M cell cycle arrest after inhibition of AURKB. The Histogram indicated the cell cycle in the H1993 and H1993 PR-S2 cells after 24 h of dose-dependent treatment with the AURKB inhibitor. The bar graph indicates the cell cycle proportion of G1, S, and G2/M.

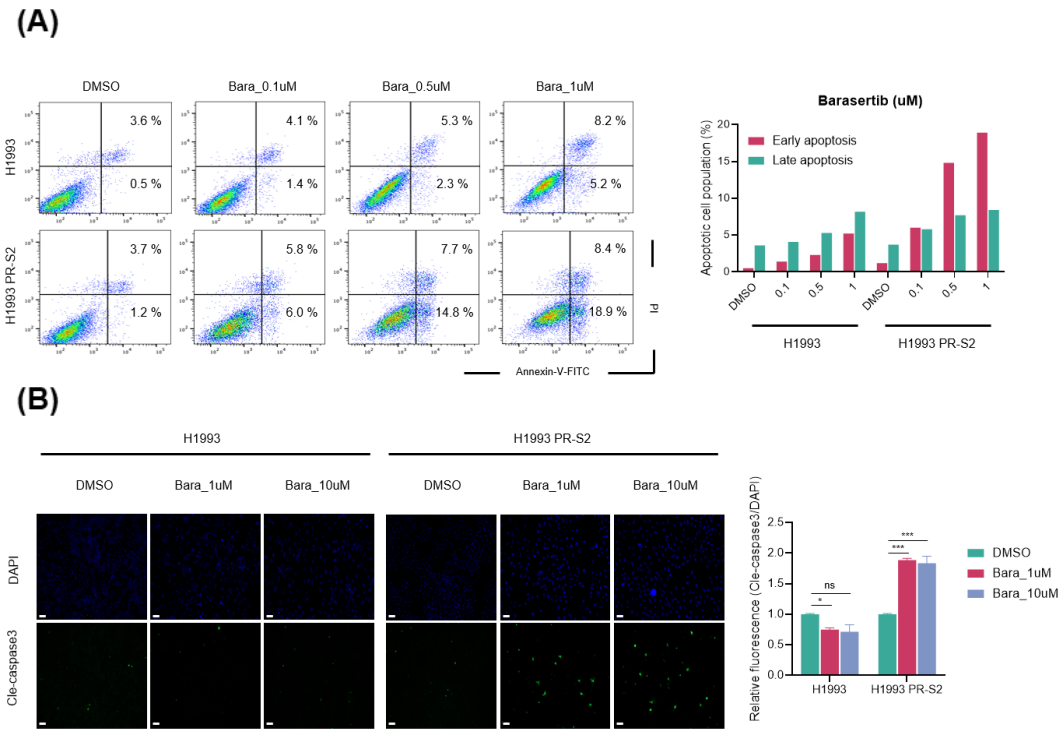

Fig 17. The apoptotic cell death after AURKB inhibitor treatment. (A) Annexin-V-FITC/PI flow cytometry analysis of the H1993 and H1993 PR-S2 cells treated with 100nM, 250nM, and 500nM of barasertib for 48 h. The bar graph represents the early and late apoptotic cell population of the barasertib-treated H1993 and H1993 PR-S2 cells. (B) Immunofluorescence analysis of nucleus (blue) and cleaved-caspase3 (green) after treatment of barasertib. Scale bars, 100 μm. The standard error of the mean (SEM) is indicated by the error bars (n = 3). Statistical analysis was performed using a two-sample t-test. ns, not significant; *p< 0.05; ***p< 0.001.

3.4. AURKB inhibition effect in various cancer cells

To substantiate the relationship between AURKB and STAT3, the impact of AURKB inhibition was evaluated in other cancer cell lines. A cell viability screening was conducted against barasertib using a collection of 18 cancer cell lines **(Fig 18A-B)**. The cancer cell lines exhibited varying sensitivities to barasertib treatment. Among the cell lines, the H460 cells, which demonstrated high sensitivity to barasertib, and the SNU-638 cells, which exhibited low sensitivity, were randomly selected. The efficacy of barasertib was then compared between the two cell lines. The results of the immunoblot analysis suggested that the inhibition of AURKB induces a reduction in the protein levels of p-STAT3 and BCL2 in the H460 cells **(Fig 19A)**. Furthermore, the proportion of cells undergoing early apoptosis was markedly elevated in barasertib-treated H460 cells compared to SNU-638 cells following Annexin-V-FITC staining using flow cytometry **(Fig 19B)**. These findings indicate that AURKB inhibition may be an effective strategy in various cancer cell lines, regardless of the MET protein level.

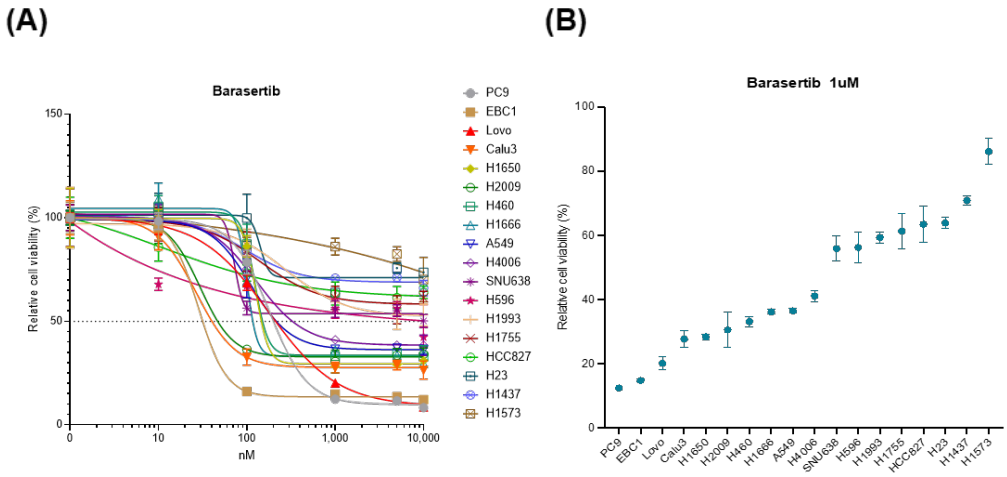

Fig 18. Various cancer cell viability screening against barasertib. Mean relative viability of various non-small cell cancer cell lines after treatment of barasertib. Cell viability with 1uM barasertib treatment is represented as a bar graph. The standard error of the mean (SEM) is indicated by the error bars.

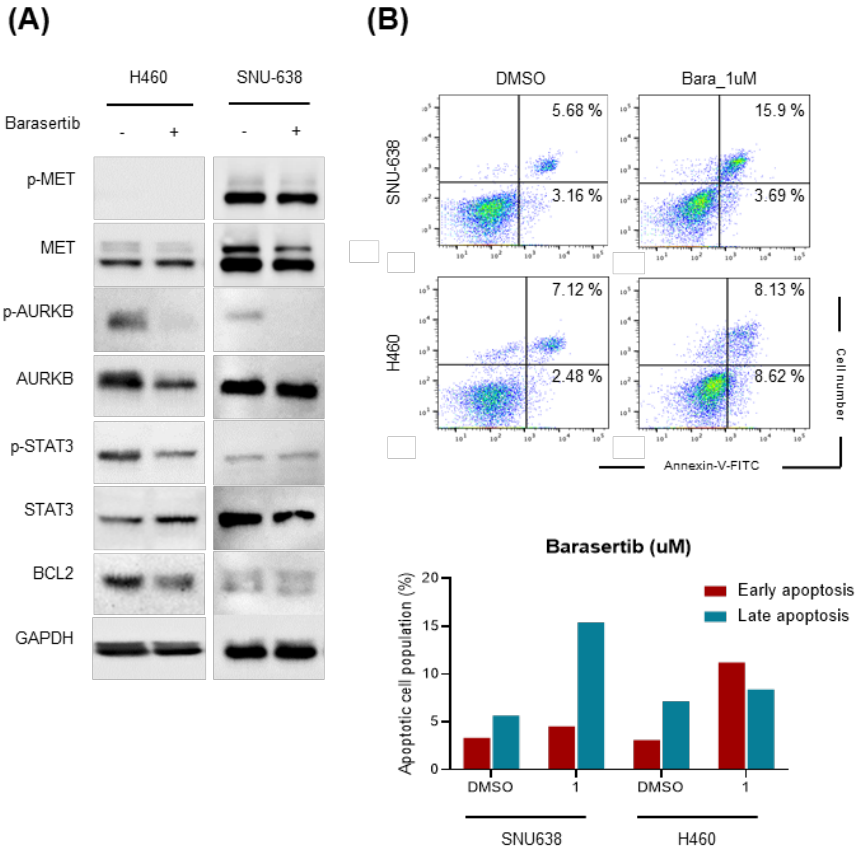

Fig 19. The AURKB inhibitor-induced STAT3 downregulation and apoptotic cell death in various cancer cell lines. (A) Immunoblot analysis of indicated primary antibodies in lower standard (H460) and higher standard (SNU-638) cell lines treatment with barasertib 1uM, 48 h. (B) Annexin-V-FITC FACs analysis of the SNU-638 and H460 cells treated with 1uM of barasertib for 48 h. The bar graph represents the early and late apoptotic cell population of the barasertib (1 uM)-treated SNU-638 and H460 cells. Abbreviation: Bara, barasertib

3.5. AURKB inhibition effect in xenograft model

The efficacy of AURKB inhibition in in vivo mouse xenograft models was subsequently validated with MET-TKI-acquired cells. Mice bearing the H1993 and the H1993 PR-S2 xenografts were treated with vehicle, PHA665752, barasertib, or a combination of both for 3 weeks **(Fig 20)**. PHA665752 treatment effectively inhibited tumor growth in the H1993 xenografts, while barasertib treatment significantly inhibited tumor growth in the H1993 PR-S2 xenografts without causing toxicity or weight loss **(Fig 21A-B and Fig 22)**. The above results were also observed in the fold change of tumor volume analysis. At the 20 days after post drug injection in *in vivo* experiments, the reduction in H1993 and H1993 PR-S2 tumor volume in each PHA665752 and barasertib group was more than twice that of the vehicle group **(Fig 21C)**. Furthermore, a notable decrease in the area of Ki-67 staining was observed in the barasertib-treated H1993 PR-S2 tumors in comparison to the vehicle-treated tumors **(Fig 23)**. The in vitro experimental evidence data were reproduced in an in vivo mouse xenograft model, which demonstrated that the AURKB inhibition can decrease cancer cell growth and ultimately lead to cell death.

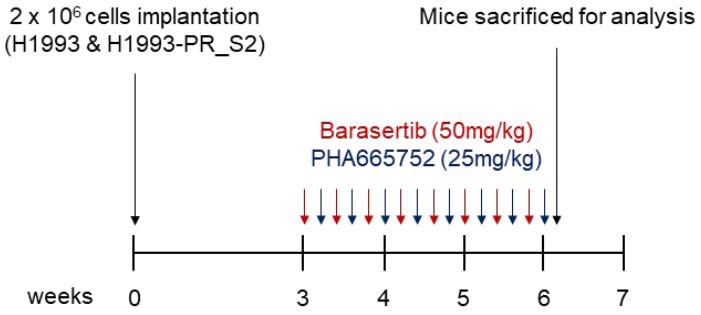

Fig 20. The strategy of in vivo experiments. Diagram summarizing xenograft strategy in NOD-2/Shi-scid IL2rgamma(null) (N2G) mice.

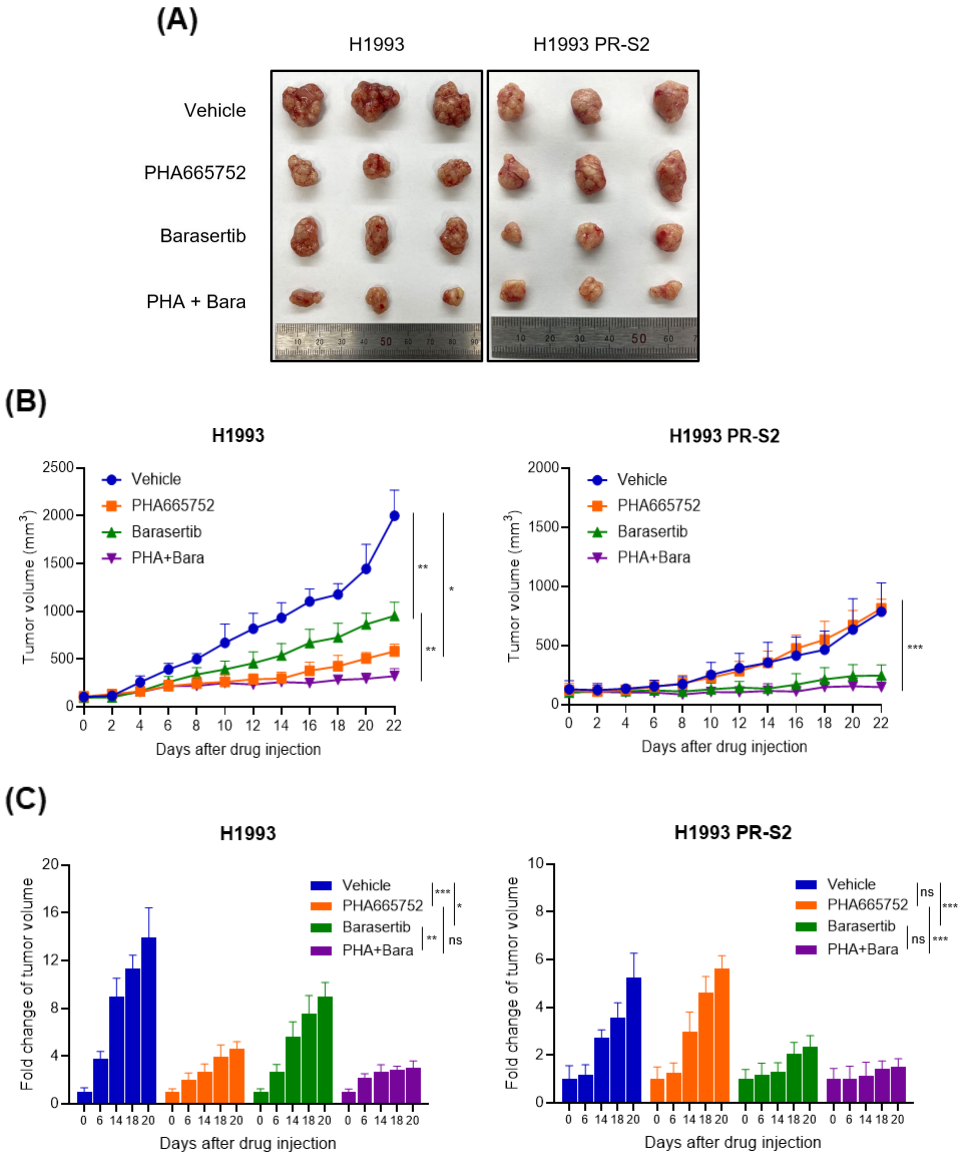

Fig 21. Xenograft tumor growth inhibition of *in vivo* mouse model. (A), (B) The measurement of tumor volume (mm3) following treatment with vehicle, PHA665752 (25 mg/kg), barasertib (50 mg/kg), and their combination for 21 days in N2G mice bearing the H1993 and H1993 PR-S2 cell

xenograft. Tumor volumes were measured twice weekly by caliper (mean ± SEM, n = 6-7 for each group). **(C)** The fold change of the tumor volume during the period of drug injection, representing 0, 6, 14, 16, 18, and 20 days. The standard error of the mean (SEM) is indicated by the error bars. Statistical analysis was performed using a two-sample t-test. ns, not significant; *p< 0.05; **p< 0.01; ***p< 0.001.

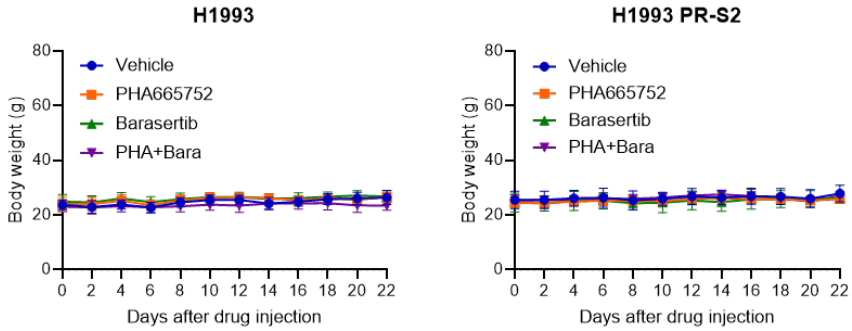

Fig 22. Body weight of *in vivo* mouse model. The body weight of each drug treatment group of mice injected with the H1993 or H1993 PR-S2 cells. The standard error of the mean (SEM) is indicated by the error bars (n = 6-7 for each group).

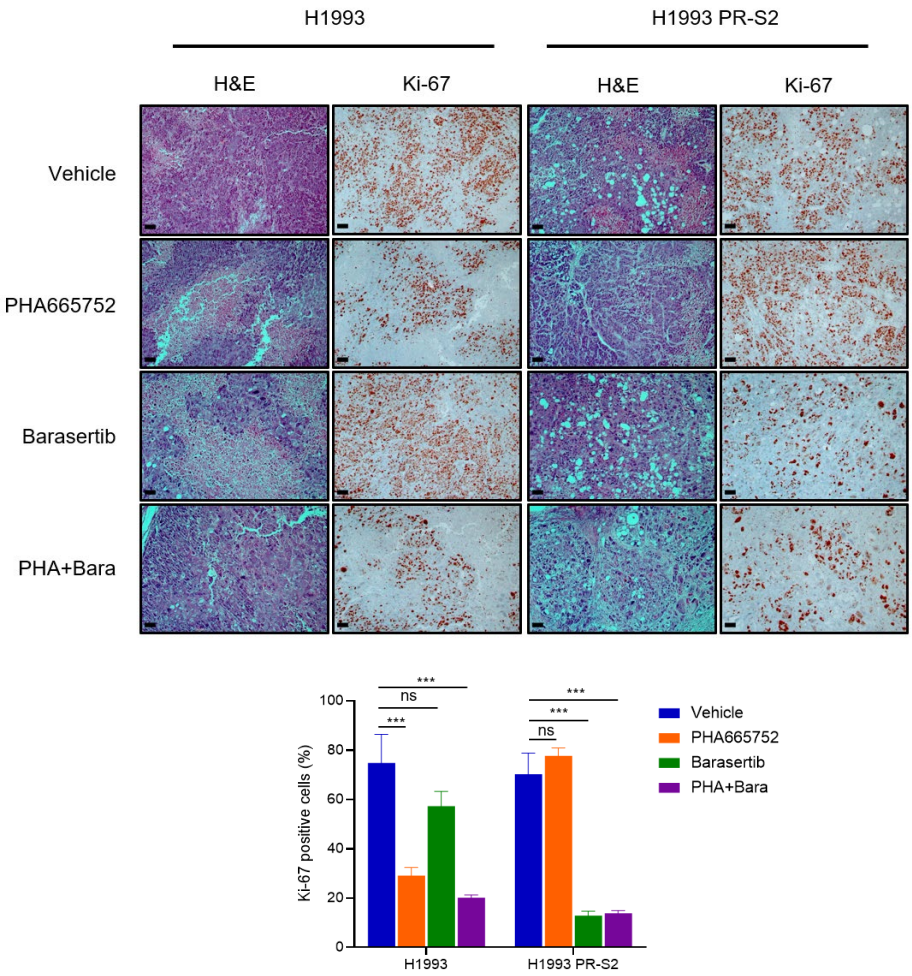

Fig 23. AURKB immunohistochemistry analysis in xenograft tumors of the H1993 and H1993 PR-S2 cells. Representative hematoxylin and eosin (H&E) and Ki-67 images of xenografts were established using either the H1993 or H1993 PR-S2 cells. Scale bars, 100 μm. The bar graph indicates the relative percentage of the Ki-67-positive cells. The standard error of the mean (SEM) is indicated by the error bars (n = 3). Statistical analysis was performed using a two-sample t-test. ns, not significant; ***p< 0.001.

3.6. AURKB expression in lung cancer with MET-TKI resistance

Finally, the aim was to ascertain whether the in vitro and in vivo findings on MET-TKI resistance with AURKB upregulation would be corroborated in patient data. Two cases were presented in which patients with advanced *MET*-amplified NSCLC had developed acquired resistance to MET-targeted therapy subsequent to an initial remarkable response. Case 1 was a 65-year-old male with advanced lung adenocarcinoma with *MET* amplification. He received 6 cycles of telisotuzumab vedotin treatment with partial response. Case 2 was a 46-year-old female with advanced lung adenocarcinoma with *MET* amplification. She received 27 cycles of ABN401 treatment with partial response. In both cases, the tumor progressed rapidly and eventually became resistant to treatment **(Table 3)**. Immunohistochemistry data of these two patients showed that AURKB protein was highly overexpressed in post-treatment samples compared to pre-treatment **(Fig 24)**.

Additionally, in the TCGA overall survival (OS) analysis, the group of lung adenocarcinoma patients with high AURKB expression exhibited significantly worse OS than the group of patients with low AURKB expression ($p = 0.0083$). So, these results supported the conclusion that high expression of AURKB can be used as a poor prognostic factor for NSCLC patients **(Fig 25)**.

Table 3. Characteristics of MET inhibitor-received *MET*-amplified non-small cell lung cancer patients.

Patient	Age/Sex	Histology	Stage	MET-amp	Drug	Cycle	Response	PFS (Mon)
Case 1	65/M	ADC	IV	Yes	Telisotuzumab vedotin	6	PR	4.6
Case 2	46/F	ADC	IV	Yes	ABN401	27	PR	18.8

Abbreviation: ADC, adenocarcinoma; MET-amp, MET-amplification; PR, Partial response; PFS, Progression-free survival

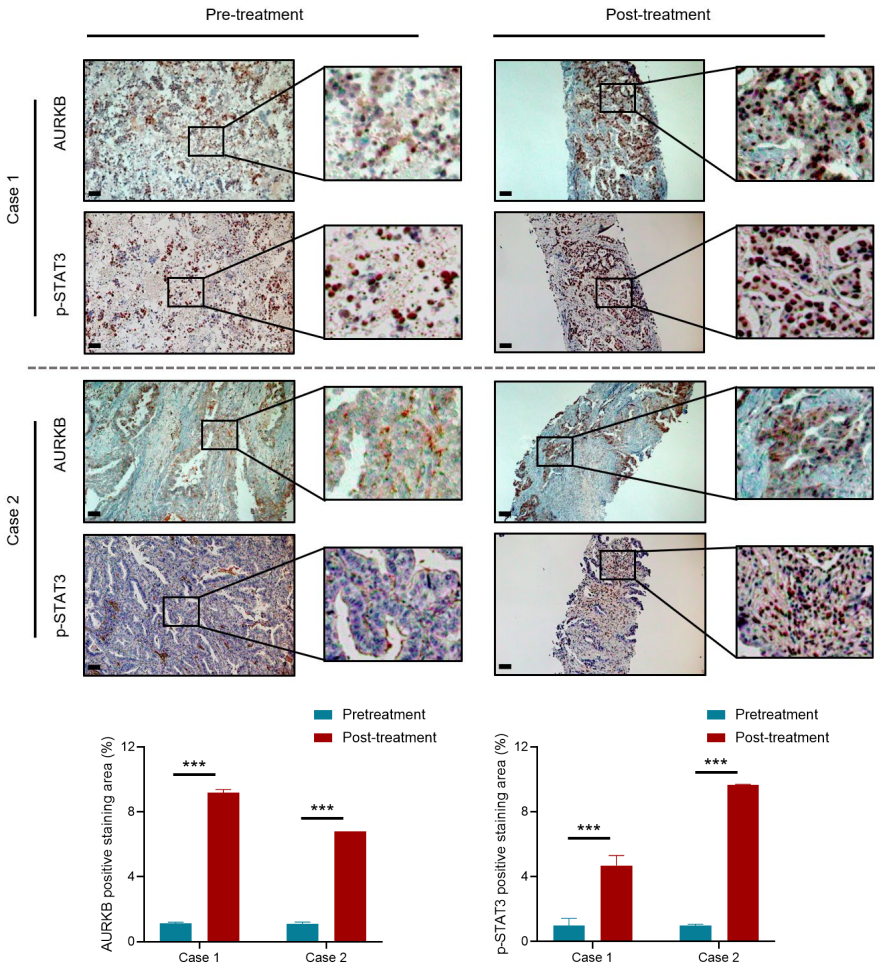

Fig 24. The immunohistochemistry of AURKB in patient samples. (A) Immunohistochemistry staining results of AURKB and p-STAT3 expression in representative two patient samples before and after MET inhibitor treatment. Scale bars, 100 μm. The bar graph indicates the relative percentage of the AURKB and p-STAT3-positive cells. The standard error of the mean (SEM) is indicated by the error bars (n = 3). Statistical analysis was performed using a two-sample t-test. ***p< 0.001.

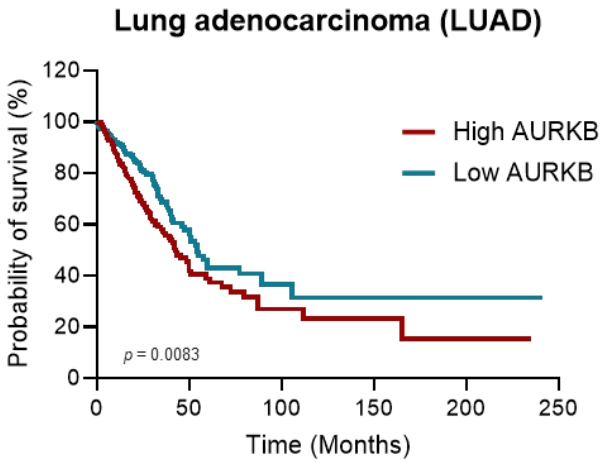

Fig 25. Kaplan-Meier survival curve of lung adenocarcinoma patients. Kaplan-Meier analysis of overall survival in LUAD patients from TCGA based on the expression of AURKB protein. Red, High AURKB expression (n = 261); Blue, low AURKB expression (n = 245). (p = 0.0083, log-rank test).

This study provides evidence that MET-TKI-acquired resistance is associated with AURKB upregulation. We found elevated AURKB protein expression in *in vitro* cell line model and showed that this elevated AURKB stimulates the STAT3/BCL2 axis and induces BIM degradation for cancer cell survival. And we showed that the MET-TKI resistance can be overcome by blocking AURKB activation, resulting in decreased expression of BCL2 and accumulation of BIM, leading to apoptotic cell death **(Fig 26)**. Taken together with *in vivo* and patient data, this study suggests that AURKB inhibition can be utilized as one of the potential therapeutic strategies to overcome MET-TKI-acquired resistance in NSCLC patients.

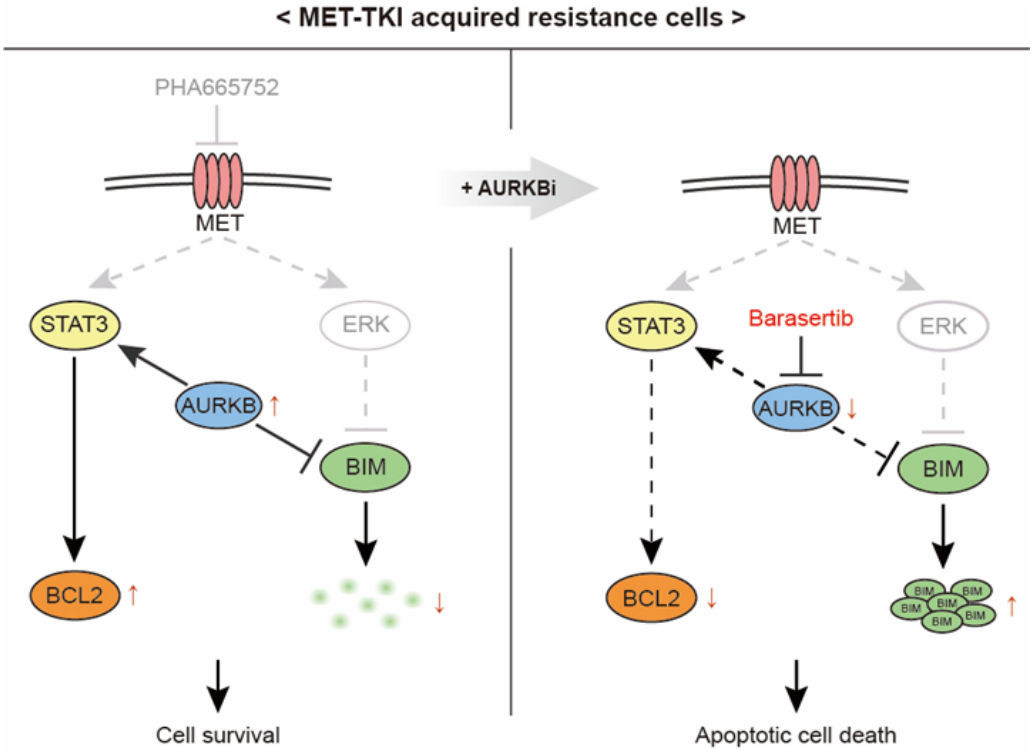

Fig 26. A schematic depicts the effects of AURKB inhibitor in MET-TKI-acquired resistance cells. During the development of the acquired resistance cell line against MET-TKI, the elevated AURKB protein has been observed. The AURKB stimulates STAT3 activation and the subsequent degradation of the pro-apoptotic protein BIM, thereby promoting cancer cell survival. The AURKB inhibitor barasertib has been demonstrated to block the phosphorylation of AURKB, which has decreased the expression of the ant-apoptotic protein BCL2 and the accumulation of BIM. Consequently, the MET-TKI-acquired resistant cells underwent apoptotic cell death via this signaling pathway.

4. DISCUSSION

Acquired drug resistance remains a significant challenge in the treatment of oncogene-addicted tumors, including MET-amplified non-small cell lung cancer (NSCLC). Despite advances in MET-targeted therapies, resistance to MET tyrosine kinase inhibitors (MET-TKIs) is inevitable, highlighting the urgent need for novel strategies to overcome this issue. Aurora kinase B (AURKB) has recently emerged as a potential target for addressing drug resistance in various cancer types. AURKB plays a crucial role in mitosis, regulating chromosome separation and cytokinesis[34]. However, its function is often dysregulated in drug-resistant cancer cells, contributing to tumor progression and therapy resistance. Several studies have implicated AURKB in promoting drug resistance. For example, AURKB overexpression has been linked to paclitaxel resistance in breast cancer cells[35] and gefitinib resistance in EGFR-mutated NSCLC cells[31]. In neuroblastoma, AURKB regulates the ERK pathway, enhancing tumorigenesis and resistance to carboplatin[36]. While these findings suggest AURKB's role in drug resistance across various cancers, its specific involvement in MET-TKI resistance in MET-amplified NSCLC has not been previously explored. Our study is the first to demonstrate that AURKB activation is critical for sustaining MET-TKI resistance in NSCLC cells. We found that AURKB mediates drug resistance by regulating the STAT3-BCL2 pathway, a key anti-apoptotic mechanism, highlighting its potential as a therapeutic target in

MET-TKI-resistant lung cancer.

In the previous study, BH3-motif subfamilies were reported that have a critical role in initiating cell survival, BIM is associated with the promotion of apoptosis[37]. There are two isoforms of BIM protein (BIM_{EL}, BIM_S)[38]. It is already known that BIM is phosphorylated by ERK1/2 kinases and regulated by ubiquitination and proteasomal degradation[39,40]. So ERK1/2 inhibition can cause BIM accumulation and lead to apoptosis. A recent study revealed that AURKB inhibition can inhibit BIM activation and lead to BIM accumulation in *EGFR*-mutated EGFR-TKI-acquired resistance NSCLC cell lines[32]. In our study, we demonstrate that increased AURKB expression inhibits BIM activation and sustains the survival of resistant NSCLC cell lines, and that this is not limited to EGFR-TKIs, but is also true in MET-amplified MET-TKI-acquired resistant NSCLC. Furthermore, inhibition of AURKB was demonstrated to reduce BIM degradation and lead accumulation in MET-amplified MET-TKI-acquired resistant NSCLC cell lines. Significantly, this study also identified a previously unreported link between MET-TKI resistance and BIM.

Although the activation of AURKB has emerged as an important drug resistance-related molecule, its upstream mechanisms are poorly understood. In this study, I try to demonstrate the direct mechanistic link between MET receptor tyrosine kinases and AURKB by investigating AURKB upstream molecular. Because the AURKB is not considered as the downstream target of MET protein as kinase, I postulated the other bypass pathway may be

involved in the AURKB-upregulated MET-TKI acquired resistance mechanism. Therefore, I focused on STAT3 activation. Among the various mechanisms of inducing STAT3 phosphorylation, the IL6/JAK axis is a major pathway of the continuous activation of STAT3 of cancer cells[41], and the IL6 receptor was already reported as a MET-TKI-acquired resistance mechanism. Because it was mentioned in the RESULT part that the phosphorylated STAT3 expression was regulated AURKB expression, the association was checked to determine whether AURKB activation is related to the IL6/JAK axis in the H1993 PR-S2 cells. However, although the protein expression of IL6 was increased in cell-grown media and cell lysate of the H1993 PR-S2 cells **(data not shown)**, there was no experimental evidence that the effect of IL6 against AURKB expression in the H1993 PR-S2 cells **(Data not shown)**. In addition, as mentioned in **Fig 9**, the JAK family expression of the H1993 PR-S2 cells was lower than that of the H1993 cells. So, these data demonstrated that AURKB-mediated STAT3 activation was not from the IL6/JAK pathway.

Although I could not suggest the direct relationship between MET receptor tyrosine kinases and AURKB, nevertheless, it is worth considering why the expression of AURKB is increased in the H1993 PR-S2 cell line that has developed resistance to MET-TKIs. As mentioned in the introduction, the downstream targets of MET receptor tyrosine kinases are diverse. The main proteins expressed are STAT3, AKT, and ERK. It is noteworthy that in the H1993 cell line used in this study, protein expression of STAT3 and ERK increased, while there was no significant

change in AKT protein expression. The generation of the H1993 PR-S2 cell line after MET-TKI treatment suggests that the survival mechanisms promoted by high levels of STAT3 and ERK are blocked. This study showed that STAT3 downstream targets, particularly BCL2, were significantly upregulated. Therefore, it can be hypothesized that this resistant cell line has evolved to conserve energy by increasing the expression of AURKB to enable survival, thereby regulating the activation of STAT3 rather than ERK as a kinase, which in turn induces activation of the BCL2-mediated apoptotic pathway.

According to Kosuke Tanaka et al., AURKB expression was upregulated in EGFR-TKI resistance NSCLC cell lines undergoing epithelial-mesenchymal transition (EMT)[32]. In this paper, the author indicates that EMT-mediated AURKB targeting is a highly effective therapy to overcome EGFR-TKI-acquired resistance in lung cancer[32]. After establishing the PHA665752-resistant cell line, increased total AURKB and p-AURKB protein expressions were observed. For this reason, the acquired resistance mechanism initially hypothesized that the EMT pathway might be related to PHA665752-induced AURKB activation. So, the immunoblot analysis was conducted, and EMT-related genes, including *ZEB1*, *SNAIL*, *VIMENTIN*, *N-CADHERIN*, and *SLUG* expressions were investigated. However, the EMT-related protein changes could not be detected in the H1993 PR-S2 cells **(Fig 27A)**. To validate this result, the VIMENTIN protein stained via immunofluorescence assay and performed a trans-well invasion assay. In the H1993 PR-S2 cells, VIMENTIN protein

expression was less detected than in the H1993 cells **(Fig 27B)**. Additionally, the H1993 PR-S2 cells exhibited a reduced invasiveness ability compared to the parental cell line, although the H1993 cells exhibited invasive properties **(Fig 27C)**. Based on these data, the results indicated that the AURKB activation of the H1993 PR-S2 cells was not from the EMT-related feature. Furthermore, it was previously reported that the AURKB pathway can be regulated by ERK activation[42]. However, the H1993 PR-S2 cells were unresponsive to several MEK inhibitors, suggesting that MET signaling has no critical role for MET-TKI resistance in these cells **(Fig 28)**. The identification of the upstream regulator of AURKB in the H1993 PR-S2 cells is a crucial step in the understanding of MET-TKI-acquired resistance. Consequently, further investigation is necessary to elucidate the mechanism underlying AURKB activation in MET-TKI-resistant NSCLC cell lines.

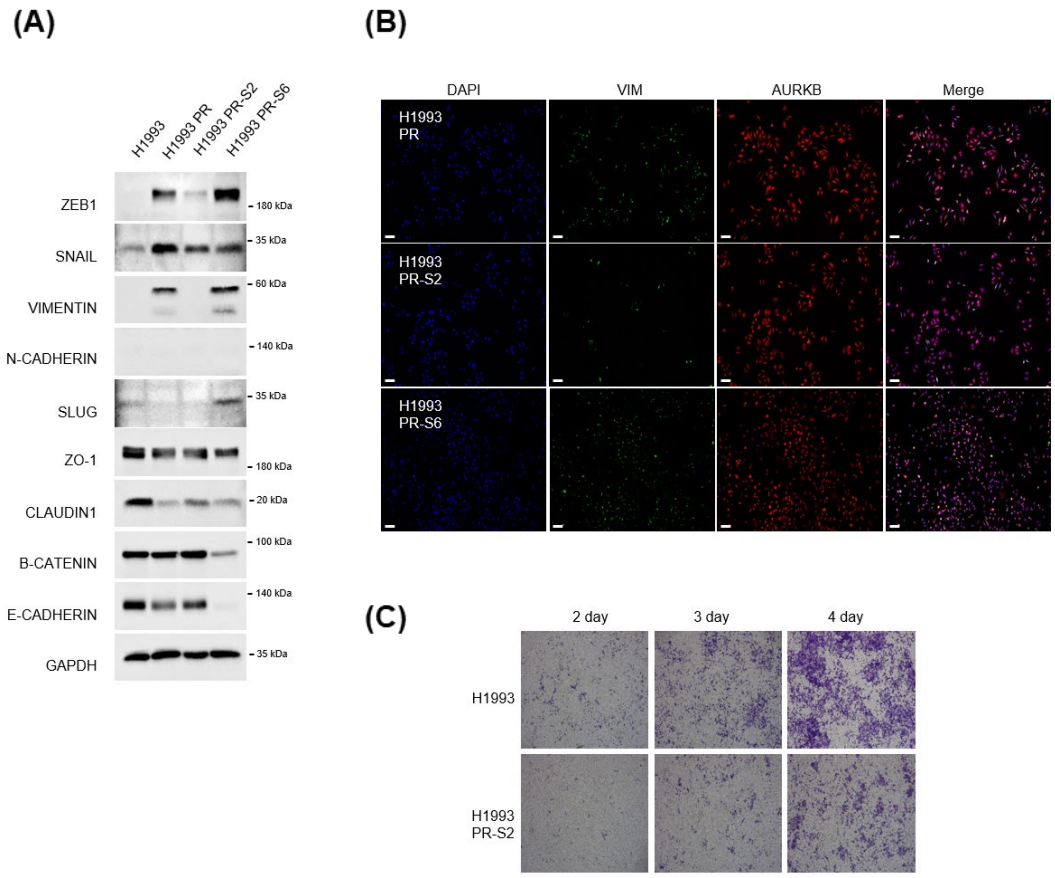

Fig 27. Analysis of EMT features in the H1993 and H1993 PR-S2 cells. (A) EMT marker and GAPDH protein expressions in parental and MET-TKI acquired resistance cell lines. (B) Immunofluorescence staining of the H1993 PR, H1993 PR-S2, and H1993 PR-S6 cells for VIMENTIN (green) and AURKB (red). Scale bars, 100 μm. (C) Representative images of trans-well assays for the H1993 cells and the H1993 PR-S2 cells.

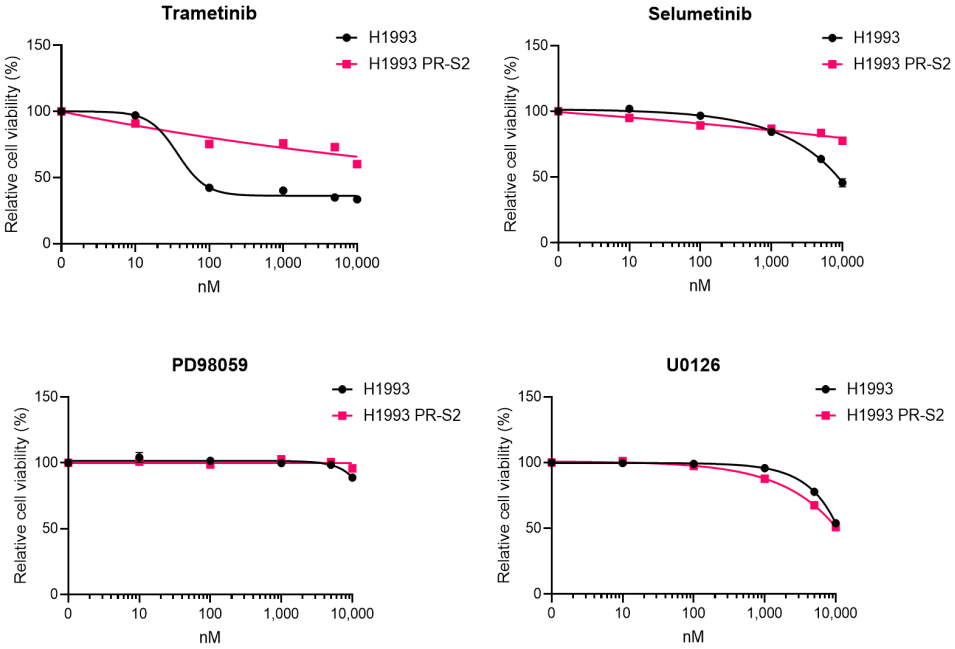

Fig 28. Inhibition effects of ERK inhibitors in the H1993 and H1993 PR-S2 cells. Mean relative cell viability of the H1993 and H1993 PR-S2 cells after treatment with trametinib, selumetinib, PD98059, and U0126.

As AURKB is overexpressed in many malignancies, inhibition of this protein by a targeted inhibitor is a central aspect of clinical trials. Over the past decade, AURKB inhibitors have been continuously developed to improve clinical efficacy. Recently, AZD2811, a modified version of AZD1152, is the most studied AURKB inhibitor in clinical trials and is being tested in two phase II trials (NCT03366675 and NCT04525391) in patients with recurrent small cell lung cancer (SCLC)[43]. Additionally, a nanoparticle-encapsulated AZD2811 was recently developed and evaluated in advanced solid tumors[44,45]. In a phase 1 trial, 51 patients were treated with nanoparticle-encapsulated AZD8211 and G-CSF (NCT02579226)[46]. The results showed that 45.1 % had disease stabilization, one patient had a partial response, and inhibition by treatment with the developed formulation of AZD8211 was well tolerated in patients with advanced solid tumors. This clinical study demonstrates the potential of inhibiting AURKB as a novel therapeutic target in lung cancer patients and we believe that our work may contribute to the groundwork for its molecular therapy development. Likewise, the development of drugs that effectively target AURKB is still ongoing. To maximize the clinical utility of AURKB inhibitors, further research is needed to identify biomarkers that can predict the efficacy of AURKB inhibitors. A previously reported preclinical article suggested that tumors with high C-MYC expression are sensitive to AURKB inhibitors[47.] The other report also showed that cell lines and xenograft tumors with high expression of BCL2 had low sensitivity to AURKB inhibitors[48]. As mentioned above, research has been conducted to identify patients who will

respond well to AURKB inhibitors. However, predictive biomarkers of AURKB efficacy remain unclear. Therefore, further molecular predictive studies are needed to support the use of AURKB inhibitors and these are clinically important for patient prognosis because they can be used as biomarkers to predict AURKB efficacy against MET-TKI resistance. A clinical evaluation of AURKB inhibitors and further study of AURKB inhibitor-sensitive prediction biomarkers will be necessary to determine the efficacy of this apoptosis-based therapeutic strategy for MET-TKI resistance lung cancer.

5. CONCLUSION

In conclusion, in this study, our molecular mechanism study confirmed that MET-TKI resistance lung cancer with *MET*-amplification uses AURKB activation for survival and regulates the STAT3/BCL2 pathway to avoid apoptosis. Additionally, we identified that inhibiting AURKB can effectively overcome this resistance induced by MET-TKI, highlighting that AURKB may be considered as one of the potential therapeutic target. Also, this study demonstrates that monotherapy of AURKB inhibitor or combination treatment with MET-TKIs may be worth exploring in clinical trials as the next-line therapy for MET-TKI-acqui red resistance NSCLC patients. Taken together, our pre-clinical research results collectively suggest that increased AURKB expression may be considered a notable biomarker in establishing a treatment strategy for MET-TKI resistance in *MET*-amplified lung cancer patients. Although the sample size of patient data was limited, we believe that our study makes a significant contribution to the literature because it elucidates a promising mechanism of drug resistance in *MET*-amplified lung cancer, a critical area of unmet need in oncology. Our findings provide a molecular basis for developing AURKB-targeted therapies, potentially improving treatment outcomes for patients with MET-TKI-resistant lung cancer.

REFERENCES

1. Livio Trusolino, Andrea Bertotti, Paolo M Comoglio. “MET Signalling: Principles and Functions in Development, Organ Regeneration and Cancer.” *Nature Reviews Molecular Cell Biology*, vol. 11, no. 12, 23 Nov. 2010, pp. 834–848.
2. Carmen Birchmeier, Walter Birchmeier, Ermanno Gherardi, George F Vande Woude. “Met, Metastasis, Motility and More.” *Nature Reviews Molecular Cell Biology*, vol. 4, no. 12, 1 Dec. 2003, pp. 915–925, www.nature.com/articles/nrm1261.
3. Ning Li, Zhangfeng Dou, Jinchun Liu, Bao Chai, Yue Li, Xiuqin An, et al. “Therapeutic Effect of HGF on NASH Mice through HGF/C-Met and JAK2-STAT3 Signalling Pathway.” *Annals of Hepatology*, vol. 17, no. 3, 1 May 2018, pp. 501–510.
4. Patrick C Ma, Maria S Tretiakova, Alexander C MacKinnon, Nithya Ramnath, Candace Johnson, Sascha Dietrich, et al. “Expression and Mutational Analysis of *MET* in Human Solid Cancers.” *Genes, Chromosomes and Cancer*, vol. 47, no. 12, Dec. 2008, pp. 1025–1037.
5. Afsane Bahrami, Soodabeh Shahidsales, Majid Khazaei, Majid Ghayour-Mobarha n, Mina Maftouh, Seyed Mahdi Hassanian, et al. “C-Met as a Potential Target for the Treatment of Gastrointestinal Cancer: Current Status and Future Perspectives.” *Journal of Cellular Physiology*, vol. 232, no. 10, 10 Apr. 2017, pp. 2657–2673.

6. Elisa Benedettini, Lynette M Sholl, Michael Peyton, John Reilly, Christopher Ware, Lenora Davis, et al. “Met Activation in Non-Small Cell Lung Cancer Is Associated with de Novo Resistance to EGFR Inhibitors and the Development of Brain Metastasis.” *The American Journal of Pathology*, vol. 177, no. 1, July 2010, pp. 415–423.

7. Pal Kaposi-Novak, Ju-Seog Lee, Luis Gòmez-Quiroz, Cédric Coulouarn, Valentina M Factor, Snorri S Thorgeirsson. “Met-Regulated Expression Signature Defines a Subset of Human Hepatocellular Carcinomas with Poor Prognosis and Aggressive Phenotype.” *Journal of Clinical Investigation*, vol. 116, no. 6, 1 June 2006, pp. 1582–1595.

8. Asaf Hellman, Eitan Zlotorynski, Stephen W Scherer, Joseph Cheung, John B Vincent, David I Smith, et al. “A Role for Common Fragile Site Induction in Amplification of Human Oncogenes.” *Cancer Cell*, vol. 1, no. 1, Feb. 2002, pp. 89–97.

9. Jae-Ho Lee, Chong Feng Gao, Chong Chou Lee, Myung Deok Kim, George F Vande Woude. “An Alternatively Spliced Form of Met Receptor Is Tumorigenic.” *Experimental & Molecular Medicine*, vol. 38, no. 5, Oct. 2006, pp. 565–573.

10. Patrick C Ma, Ramasamy Jagadeeswaran, Simha Jagadeesh, Maria S Tretiakova, Vidya Nallasura, Edward A Fox, et al. “Functional Expression and Mutations of C-Met and Its Therapeutic Inhibition with SU11274 and Small Interfering RNA in Non-Small Cell Lung Cancer.” *Cancer Research*, vol. 65, no. 4, 15 Feb. 2005, pp. 1479–1488.

11. Francisco Sanchez-Vega, Marco Mina, Joshua Armenia, Walid K Chatila, Augustin Luna, Konnor C La, et al. “Oncogenic Signaling Pathways in the Cancer Genome Atlas.” *Cell*, vol. 173, no. 2, Apr. 2018, pp. 321-337.e10.

12. Kyle Ellrott, Matthew H Bailey, Gordon Saksena, Kyle R Covington, Cyriac Kandoth, Chip Stewart, et al. “Scalable Open Science Approach for Mutation Calling of Tumor Exomes Using Multiple Genomic Pipelines.” *Cell Systems*, vol. 6, no. 3, 28 Mar. 2018, pp. 271-281.e7.

13. Garrett M Frampton, Siraj M Ali, Mark Rosenzweig, Juliann Chmielecki, Xinyuan Lu, Todd M Bauer, et al. “Activation of MET via Diverse Exon 14 Splicing Alterations Occurs in Multiple Tumor Types and Confers Clinical Sensitivity to MET Inhibitors.” *Cancer Discovery*, vol. 5, no. 8, 1 Aug. 2015, pp. 850–859.

14. Ana C Z Gelatti, Alexander Drilon, Fernando C Santini. “Optimizing the Sequencing of Tyrosine Kinase Inhibitors (TKIs) in Epidermal Growth Factor Receptor (EGFR) Mutation-Positive Non-Small Cell Lung Cancer (NSCLC).” *Lung Cancer*, vol. 137, no. 137:113-122., Nov. 2019, pp. 113–122.

15. Joanna H Tong, Sai F Yeung, Anthony W H Chan, Lau Y Chung, Shuk L Chau, Raymond Wai Ming Lung, et al. “MET Amplification and Exon 14 Splice Site Mutation Define Unique Molecular Subgroups of Non-Small Cell Lung Carcinoma with Poor Prognosis.” *Clinical Cancer Research*, vol. 22, no. 12, 4 Feb. 2016, pp.

3048–3056.

16. Yan Feng, Patrick C Ma. “MET Targeted Therapy for Lung Cancer: Clinical Development and Future Directions.” *Lung Cancer: Targets and Therapy*, vol. 9;3:53-67, no. 2012 Aug 9;3:53-67.
17. Xiangdong Liu, Qian Wang, Gengjie Yang, Cindy Marando, Holly K Koblish, Leslie M Hall, et al. “A Novel Kinase Inhibitor, INCB28060, Blocks C-MET–Dependent Signaling, Neoplastic Activities, and Cross-Talk with EGFR and HER-3.” *Clinical Cancer Research*, vol. 17, no. 22, 14 Sept. 2011, pp. 7127–7138.
18. Sabrina Baltschukat, Barbara Schacher Engstler, Alan Huang, Huai-Xiang Hao, Angela Tam, Hui Qin Wang, et al. “Capmatinib (INC280) Is Active against Models of Non–Small Cell Lung Cancer and Other Cancer Types with Defined Mechanisms of MET Activation.” *Clinical Cancer Research*, vol. 25, no. 10, 23 Jan. 2019, pp. 3164–3175.
19. Jürgen Wolf, Takashi Seto, Ji-Youn Han, Noemi Reguart, Edward B Garon, Harry J M Groen, et al. “Capmatinib in MET Exon 14–Mutated or MET-Amplified Non–Small-Cell Lung Cancer.” *New England Journal of Medicine*, vol. 383, no. 10, 3 Sept. 2020, pp. 944–957.
20. Paul K Paik, Enriqueta Felip, Remi Veillon, Hiroshi Sakai, Alexis B Cortot, Marina C Garassino, et al. “Tepotinib in Non–Small-Cell Lung Cancer with MET Exon 14

Skipping Mutations.” *New England Journal of Medicine*, vol. 383, no. 10, 3 Sept. 2020, pp. 931–943.

21. Toshio Fujino, Kenichi Suda, Takamasa Koga, Akira Hamada, Shuta Ohara, Masato Chiba, et al. “Foretinib Can Overcome Common On-Target Resistance Mutations after Capmatinib/Tepotinib Treatment in NSCLCs with MET Exon 14 Skipping Mutation.” *Journal of Hematology & Oncology*, vol. 15, no. 1, 11 June 2022.
22. Ralph Tiedt, Elisa Degenkolbe, Pascal Furet, Brent A Appleton, Sabrina Wagner, Joseph Schoepfer, et al. “A Drug Resistance Screen Using a Selective MET Inhibitor Reveals a Spectrum of Mutations That Partially Overlap with Activating Mutations Found in Cancer Patients.” *Cancer Research*, vol. 71, no. 15, 1 Aug. 2011, pp. 5255–5264.
23. Toshio Fujino, Yoshihisa Kobayashi, Kenichi Suda, Takamasa Koga, Masaya Nishino, Shuta Ohara, et al. “Sensitivity and Resistance of MET Exon 14 Mutations in Lung Cancer to Eight MET Tyrosine Kinase Inhibitors in Vitro.” *Thorac Oncol.* , vol. 14, no. 10, 1 Oct. 2019, pp. 1753–1765.
24. Lars D Engstrom, Ruth Aranda, Matthew Lee, Elizabeth A Tovar, Curt J Essenburg, Zachary Madaj, et al. “Glesatinib Exhibits Antitumor Activity in Lung Cancer Models and Patients Harboring *MET* Exon 14 Mutations and Overcomes Mutation-Mediated Resistance to Type I MET Inhibitors in Nonclinical Models.” *Clinical Cancer Research*, vol. 23, no. 21, 31 Oct. 2017, pp. 6661–6672.

25. Gonzalo Recondo, Magda Bahcall, Liam F Spurr, Jianwei Che, Biagio Ricciuti, Giulia C Leonardi, et al. “Molecular Mechanisms of Acquired Resistance to MET Tyrosine Kinase Inhibitors in Patients with MET Exon 14–Mutant NSCLC.” *Clin Cancer Res.* , vol. 26, no. 11, 7 Feb. 2020, pp. 2615–2625.

26. Yunqing Li, Fadila Guessous, Elizabeth B Johnson, Charles G Eberhart, Xiao-Nan Li, Qing Shu, et al. “Functional and Molecular Interactions between the HGF/C-Met Pathway and C-Myc in Large-Cell Medulloblastoma.” *Laboratory Investigation*, vol. 88, no. 2, 1 Feb. 2008, pp. 98–111.

27. Ken Suzawa, Michael Offin, Daniel Lu, Christopher Kurzatkowski, Morana Vojni c, Roger S Smith, et al. “Activation of KRAS Mediates Resistance to Targeted Therapy in MET Exon 14–Mutant Non–Small Cell Lung Cancer.” *Clin Cancer Res*, vol. 25, no. 4, 15 Feb. 2019, pp. 1248–1260.

28. Wenzhong Que, Junmin Chen, Ma Chuang, Danrong Jiang, et al. “Knockdown of C-Met Enhances Sensitivity to Bortezomib in Human Multiple Myeloma U266 Cells via Inhibiting Akt/MTOR Activity.” *APMIS*, vol. 120, no. 3, 11 Nov. 2011, pp. 195–203.

29. Mathieu Chevallier, Maxime Borgeaud, Alfredo Addeo, Alex Friedlaender. “Oncogenic Driver Mutations in Non-Small Cell Lung Cancer: Past, Present and Future.” *World Journal of Clinical Oncology*, vol. 12, no. 4, 24 Apr. 2021, pp. 217–237.

30. Hidemasa Goto, Yoshihiro Yasui, Erich A Nigg, Masaki Inagaki, et al. “Aurora-B

Phosphorylates Histone H3 at Serine28 with Regard to the Mitotic Chromosome Condensation." *Genes to Cells*, vol. 7, no. 1, Jan. 2002, pp. 11–17.

31. Jordi Bertran-Alamillo, Valérie Cattan, Marie Schoumacher, Jordi Codony-Servat, Ana Giménez-Capitán, Frédérique Cantero, et al. "AURKB as a Target in Non-Small Cell Lung Cancer with Acquired Resistance to Anti-EGFR Therapy." *Nature Communications*, vol. 10, no. 1, 18 Apr. 2019.
32. Kosuke Tanaka, Helena A Yu, Shaoyuan Yang, Song Han, S Duygu Selcukl u, Kwanghee Kim, et al. "Targeting Aurora B Kinase Prevents and Overcomes Resistance to EGFR Inhibitors in Lung Cancer by Enhancing BIM- and PUMA-Mediated Apoptosis." *Cancer Cell*, vol. 39, no. 9, Sept. 2021, pp. 1245-1261.e6.
33. Robert W Wilkinson, Rajesh Odedra, Simon P Heaton, Stephen R Wedge, Nicholas J Keen, Claire Crafter, et al. "AZD1152, a Selective Inhibitor of Aurora B Kinase, Inhibits Human Tumor Xenograft Growth by Inducing Apoptosis." *Clinical Cancer Research*, vol. 13, no. 12, 15 June 2007, pp. 3682–3688.
34. D M Glover, M H Leibowitz, D A McLean, H Parry. "Mutations in Aurora Prevent Centrosome Separation Leading to the Formation of Monopolar Spindles." *Cell*, vol. 81, no. 1, Apr. 1995, pp. 95–105.
35. Min Liu, Yinan Li, Cui Zhang, Qing Zhang. "Role of Aurora Kinase B in Regulating Resistance to Paclitaxel in Breast Cancer Cells." *Human Cell*, vol. 35, no. 2, 28 Jan.

2022, pp. 678–693.

36. Yonglin Yang, Ying Sheng, Dahong Sun, Jilan Sun, Li Li, Lizhi Sun. “AURKB Promotes Tumorigenesis and Carboplatin Resistance by Regulating the ERK Pathway in Neuroblastoma Cells.” *International Journal of Neuroscience*, vol. 133, no. 11, 17 July 2023, pp. 1224–1232.
37. Jerry M Adams. “Ways of Dying: Multiple Pathways to Apoptosis.” *Genes & Development*, vol. 17, no. 20, 15 Oct. 2003, pp. 2481–2495.
38. L O'Connor, A Strasser, L A O'Reilly, G Hausmann, J M Adams, S Cory, et al. “Bim: A Novel Member of the Bcl-2 Family That Promotes Apoptosis.” *The EMBO Journal*, vol. 17, no. 2, 15 Jan. 1998, pp. 384–395.
39. Toru Akiyama, Phillippe Bouillet, Tsuyoshi Miyazaki, Yuho Kadono, Hirotaka Chikuda, Ung-Il Chung, et al. “Regulation of Osteoclast Apoptosis by Ubiquitylation of Proapoptotic BH3-Only Bcl-2 Family Member Bim.” *The EMBO Journal*, vol. 22, no. 24, 15 Dec. 2003, pp. 6653–6664.
40. Rebecca Ley, Kathryn Balmanno, Kathryn Hadfield, Claire Weston, Simon J Cook. “Activation of the ERK1/2 Signaling Pathway Promotes Phosphorylation and Proteasome-Dependent Degradation of the BH3-Only Protein, Bim.” *Journal of Biological Chemistry*, vol. 278, no. 21, 19 Mar. 2003, pp. 18811–18816.
41. Hua Yu, Marcin Kortylewski, Drew Pardoll. “Crosstalk between Cancer and Immune

Cells: Role of STAT3 in the Tumour Microenvironment." *Nature Reviews Immunology*, vol. 7, no. 1, Jan. 2007, pp. 41–51.

42. Bonet C, Giuliano S, Ohanna M, Bille K, Allegra M, Lacour JP, et al. "Aurora B is regulated by the mitogen-activated protein kinase/extracellular signal-regulated kinase (MAPK/ERK) signaling pathway and is a valuable potential target in melanoma cells." *J Biol Chem*, vol. 287, no. 35, Aug. 2012, pp. 29887–29898.
43. Sehhoon Park, Joonho Shim, Peter G S Mortimer, Simon A Smith, Robert E Godi n, Simon J Hollingsworth, et al. "Biomarker-Driven Phase 2 Umbrella Trial Study for Patients with Recurrent Small Cell Lung Cancer Failing Platinum-Based Chemotherapy." *Cancer*, vol. 126, no. 17, 25 June 2020, pp. 4002–4012.
44. Young Ho Song, Eyoung Shin, Hong Wang, Jim Nolan, Susan Low, Donald Parsons, et al. "A Novel in Situ Hydrophobic Ion Pairing (HIP) Formulation Strategy for Clinical Product Selection of a Nanoparticle Drug Delivery System." *Journal of Controlled Release*, vol. 229, no. 2016;229:106-19., May 2016, pp. 106–119.
45. Susan Ashton, Young Ho Song, Jim Nolan, Elaine Cadogan, Jim Murray, Rajesh Odedra, et al. "Aurora Kinase Inhibitor Nanoparticles Target Tumors with Favorable Therapeutic Index in Vivo." *Science Translational Medicine*, vol. 8, no. 325, 10 Feb. 2016, pp. 325ra17–325ra17.
46. Melissa L Johnson, Judy S Wang, Gerald Falchook, Carol Greenlees, Suzanne

Jones, Donald Strickland, et al. “Safety, Tolerability, and Pharmacokinetics of Aurora Kinase B Inhibitor AZD2811: A Phase 1 Dose-Finding Study in Patients with Advanced Solid Tumours.” *British Journal of Cancer*, vol. 128, no. 10, 4 Mar. 2023, pp. 1906–1915.

47. Barbara A Helfrich, Jihye Kim, Dexiang Gao, Daniel C Chan, Zhiyong Zhan g, Aik-Choon Tan, et al. “Barasertib (AZD1152), a Small Molecule Aurora B Inhibitor, Inhibits the Growth of SCLC Cell Lines *in Vitro* and *in Vivo*.” *Molecular Cancer Therapeutics*, vol. 15, no. 10, 1 Oct. 2016, pp. 2314–2322.
48. Kavya Ramkumar, Azusa Tanimoto, Carminia M Della Corte, C Allison Stewart, Qi Wang, Li Shen, et al. “Targeting BCL2 Overcomes Resistance and Augments Response to Aurora Kinase B Inhibition by AZD2811 in Small Cell Lung Cancer.” *Clinical Cancer Research*, vol. 29, no. 16, 8 June 2023, pp. 3237–3249.

< ABSTRACT(IN KOREAN)>

오로라 키나아제 B 억제를 통한 MET 증폭 폐암의 MET 표적 약물 내성 극복 메커니즘 연구

MET 증폭 폐암 환자에서 MET 표적 치료제에 대한 내성은 치료 효과를 제한하는 주요 요인으로, 이를 극복할 수 있는 새로운 치료 전략의 개발이 필수적이다. 본 연구에서는 MET 억제제에 대한 비유전체적 내성 메커니즘을 규명하고, 후보 억제제의 항종양 효과를 다양한 종양 모델에서 평가하였다.

MET 증폭 폐암 세포주(H1993)에 MET 억제제인 PHA665752를 장기적으로 처리하여 내성 세포주(H1993 PR-S2)를 확립하였으며, 약물화 가능한 억제제 라이브러리를 활용한 고처리량 스크리닝(HTS)을 통해 유망한 후보 약물을 선별하였다. 그 결과, 오로라 B(AURKB) 억제제인 바라서팁(barasertib)이 내성 세포에서 유의미한 성장 억제 효과를 보임을 확인하였다. H1993 PR-S2 세포에서는 p-AURKB의 발현이 증가하였으며, 그 하위 분자인 Histone H3의 발현에는 변화가 없었다. 반면, p-STAT3 및 항세포사멸 유전자 BCL2의 발현은 현저히 증가하였다. 바라서팁 처리 시, p-STAT3와 BCL2 발현은 감소하고 세포사멸 유도 유전자인 BIM의 축적이 관찰되었으며, 내성 세포에서 G2/M 세포주기 정지 및 세포사멸이 유도되었다. 이러한 효과는 다양한 암 세포주와 마우스 이종이식 모델에서도 재현되었다.

또한, MET 억제제 내성을 획득한 환자의 면역조직화학 분석 결과, 치료 전보다 치료 후 종양에서 AURKB의 발현이 유의하게 증가하였으며, TCGA 데이터 분석을 통해 AURKB 발현이 높은 폐암 환자군이 낮은 환자군에 비해 불량한 예후를 보이는

것으로 나타났다.

종합하면, 본 연구는 MET 억제제 내성 폐암 세포가 AURKB 활성화 및 STAT3/BCL2 신호 전달 경로를 통해 우회적 생존 메커니즘을 활용함을 제시하며, AURKB 억제를 통해 이러한 우회 경로를 차단함으로써 AURKB 저해제가 내성 극복을 위한 유효하고 실질적인 임상적 대안이 될 수 있음을 강하게 시사한다. 이러한 결과는 MET 억제제 내성 환자에 대한 치료 전략 개발에 핵심적인 단서를 제공하며, 더 나아가 향후 AURKB 기반 임상 연구의 과학적 근거로 활용될 수 있을 것이다.

핵심되는 말 : 폐암, 표적치료, MET 증폭 폐암, 항암제, 항암 내성